Spring 2016

Characterization Of The Skeletal Phenotype In Idua-W392X Knock-In Mice: Bone Metabolism Biomarkers

Christina J. Owensby

CHARACTERIZATION OF THE SKELETAL PHENOTYPE IN IDUAW392X KNOCK-IN MICE: BONE METABOLISM BIOMARKERS

A Masters Thesis

Presented to

The Graduate College of

Missouri State University

In Partial Fulfillment

Of the Requirements for the Degree

Master of Science, Cell and Molecular Biology

By

Christina J. Owensby

May 2016

CHARACTERIZATION OF THE SKELETAL PHENOTYPE IN IDUAW392X KNOCK-IN MICE: ANALYZING BONE METABOLISM BIOMARKERS

Biomedical Sciences

Missouri State University, May 2016

Master of Science

Christina J. Owensby

ABSTRACT

Mucopolysaccharidosis Type I (MPS I, Hurlers Syndrome) is a lysosomal storage disease caused by a deficiency of alpha-L-iduronidase (IDUA). IDUA catalyzes the degradation of the two glycosaminoglycans (GAGs); heparin sulfate (HS) and demantan sulfate (DS). The accumulation of HS and DS makes MPS I progressive with inevitable degeneration of multiple organ systems. Accumulated excess of GAGs on the skeletal system causes dysostosis multiplex, atlantoaxial instability, thoracolumbar kyphosis, genu valgum, acetabular dysplasia, and short stature. Skeletal biomarkers of bone formation and bone resorption were compared in wild-type, heterozygous, and IDUAW392X mice. To investigate osteoblast activity, levels of the bone formation marker Procollagen type I N-terminal propeptide (PINP) were evaluated. To investigate osteoclast activity, levels of the bone resorption biomarker Tartrate-resistant acid phosphatase (TRAP5b) were evaluated. Potential differences in serum PINP or serum TRAP5b concentrations could contribute to the increased cortical thickness and increased bone marrow width seen in the skeletal phenotype previously identified in mice with IDUA deficiency. Lastly to further investigate bone metabolism, transcription of six biomarkers were quantified: collagen (I), RANKL, OPG, TNFα, and CSF-1 isolated from tibiae of wild type, heterozygous, and DUAW392X mice. No significant differences were found between the genotypes for PINP, TRAP5b, and transcription levels of type I collagen. Lower transcriptional levels were found for RANKL, OPG, TNFα and CSF-1 for IDUA deficient mice compared to wild-type mice.

KEYWORDS: mucopolysaccardosis, Hurlers syndrome, lysosomal storage disorder, α-L-iduronidase bone remodeling, bone resorption, bone formation, PINP, TRAP5b

This abstract is approved as to form and content:

_____

Amanda C. Brodeur
Chairperson, Advisory Committee
Missouri State University

CHARACTERIZATION OF THE SKELETAL PHENOTYPE IN IDUAW392X KNOCK-IN MICE: ANALYZING BONE METABOLISM BIOMARKERS

By

Christina J. Owensby

A Master's Thesis
Submitted to the Graduate College
Of Missouri State University
In Partial Fulfillment of the Requirements
For the Degree of Master of Science, Cell and Molecular Biology

May 2016

Approved:

_____
Dr. Amanda C. Brodeur

_____
Dr. Joshua J. Smith

_____
Dr. Ben Timson

_____
Dr. Julie Masterson, Dean, Graduate College

ACKNOWLEDGEMENTS

I would like to thank the following people for their support during the course of my graduate studies. First, I want to thank the undergraduate students assisted in the ELISA experiments, they include Jay Guyll, Sarah Carney, Kristie Leslie, Natalie Picciano, and Peter Wittl.

Second, I owe Dr. Todd Daniel and Jahnavi Delmonico on the RSTATS team at Missouri State University for providing their knowledge on statistical testing for PINP.

I want to thank Dr. Charlotte Phillips, Arin Kettle Osetreich and Jeong J. Young for welcoming me into their lab at the University of Missouri to complete the RNA isolation from bone and RT-PCR. I would like to thank Arin Kettle Osetreich for providing me with her valuable advice on experimental design and analysis.

I also want to thank my committee members, Dr. Joshua J. Smith for his guidance in lab work and Dr. Ben Timson for his commitment to challenging my perspectives on education.

Notably, this would not be possible if it was not for the continued support from my advisor, Dr. Amanda Brodeur. From whom I have learn a great deal. I appreciate the guidance she has provided over the last two years.

TABLE OF CONTENTS

LIST OF TABLES

LIST OF FIGURES

INTRODUCTION

Mucopolysaccharidosis Type I

Mucopolysaccharidosis Type I (MPS I, Hurlers Syndrome) is a lysosomal storage disorder caused by a deficiency of α-L-iduronidase (IDUA). IDUA catalyzes the degradation of the glycosaminoglycans (GAGs), heparin sulfate (HS) and dermatan sulfate (DS)**.** The continual accumulation of HS and DS makes MPS I a progressive disease with inevitable degeneration of multiple organ systems (Bach et al, 1972), affecting respiratory, cardiac, skeletal, ophthalmologic, and in some cases central nervous system function. The effect of accumulated GAGs on the skeletal system includes dysostosis multiplex, atlantoaxial instability, thoracolumbar kyphosis, genu valgum, acetabular dysplasia, and short statute. Historically, MPS I has been categorized into three phenotypic subtypes: Hurlers syndrome designates the severe form, Hurler-Scheie the intermediate form, and Scheie the attenuated form (Table 1).

Glycosaminoglycans (GAGs) have two structural parts: a proteoglycan core and chains of repeating disaccharide units. The proteoglycan core consists of a serine residue attached to a glycine residue. The glycine acts as a linker protein between the serine residue and the repeating disaccharide units (Prydz K. 2015). The basic structure of glycosaminoglycans chains are alternating repeats of an iduronic acid (IdoA) residues and an amino sugar residue. The specific roles of a GAG is dependent on the complexity of the modifications of the chains. The specific patterns of epimerization and sulfation along GAG chains promote specific interactions with growth factors helping regulate growth, development, differentiation and immunological mechanisms (Prydz K. 2015).

Table One: Disease Heterogenerity

Form	Severity	Description
Hurler's Syndrome	High	Early on-set rapidly progressive, neurodegenerative
Hurler-Scheie's Syndrome	Intermediate	Onset and progression between Hurler and Scheie extremes, with mild or absent central nervous system involvement
Scheie's Syndrome	Mild	later onset, less rapid progression, no neurodegeneration

A more detailed structure of HS chains consists of repeating disaccharides of *N*-acetyl-d-glucosamine (GlcNAc) and d-gucuronic acid (GlcUA) or L-iduronic acid (IdoUA) (Mizumoto S. et al 2015). Higher sulfated regions of HS are known to interact with growth factors and extracellular matrix molecules (Yoneda, A. 2012). Also, hydrated GAG gels have been known to play an important role for the absorption of pressure changes in joints and tissues (Prydz K. 2015). DS is composed of the same core protein but attached to *N*-acetyl-d-galactosamine (GalNAc) and L-iduronic acid (IdoUA) (Mizumoto S. et al 2015). DS is known to be an anticoagulant and antithrombotic glycosaminoglycan.

In Hurler Syndrome, disease heterogeneity is a result of specific mutations leading to varying levels of residual activity of IDUA and accumulation level of HS and DS. The lower the residual activity of IDUA results in a higher severity. Without treatment a patient with Hurlers Syndrome will not have a life span extending past childhood; however the available treatment options have increased life span to early adulthood. Currently, MPS I treatments include: enzyme replacement therapy (ERT), bone marrow or umbilical cord stem cell transplantation, and corrective surgery.

Treatment Options for Mucopolysaccharidosis Type I

ERT is the use of recombinant human alpha-L-iduronidase, Laronidase, to simulate IDUA activity to degrade HS and DS. Laronidase was approved for treatment of the attenuated form of MPS I in the UK and Europe in 2004 after successful Phase III clinical trials. It significantly improves respiratory function and physical capacity, as well as reduces glycosaminoglycan storage (Wraith J.E. et al, 2005). The recombinant enzyme

is unable to cross the blood-brain barrier making it incapable of reducing the neuropathology of MPS1-H. This is not an area of concern for treatment of attenuated forms, since central nervous system manifestations are not observed. An inhibitory antibody (IgG) response to Laronidase has been observed, raising the concern as to if serial, life-long infusions of the recombinant protein will remain efficacious (Tolar J and Orchard P. 2008). In double-blind, placebo-controlled trials of laronidase, 53% of the 46 patients had infusion-associated reactions, however they were considered to be mild, easily managed and decreased markedly after 6 months (Wraith J.E. et al 2004). Immunosuppressants, cyclosporine and azathioprine, have been seen to be successful to reduce the immune response (Kakkis et al 2004). Despite the available studies demonstrating ERT to be safe and efficacious, the long-term impact of ERT remains unknown (Coman D.J. et al 2008). Additionally, laronidase is not successful in treating the bone abnormalities in MPS I due to unknown barriers (Wraith J.E.2006).

Benefits of ERT. In a 26-week, double-blind, placebo-controlled trial of laronidase were enrolled in a 3.5-year open-label extension study, patients with the attenuate form showed improvement in sleep apnea and increase shoulder fexion after infusions with Laronidase (Wraith J.E. et al 2004). Improvement was noted in the mobility of MPS I demonstrated in the of the 6min-walk test (6MWT), alongside decrease GAG content found in the urinary system and liver.

Hematopoietic Stem Cell Transplantation (HSCT). HSCT is currently the most effective treatment for the more serve forms of MPS I. Bone Marrow Transplantation (BMT) has been used to treat MPS1-H since the first treatment in 1981 (Hobbs J.R. et al 1981). The donor cells, taken from bone marrow or umbilical cord blood of unrelated

donors, secrete a functional α-L-iduronidase, capable of crossing the blood brain barrier to treat the neuropathology found in MPS1-H. The IDUA secreted from donor cells are able to cross the cellular membranes in recipient cells by the addition of a mannose-6-phosphate residue (Hasilik A and Neufeld E 1980). After internalization, donor IDUA is directed to lysosomes in order to take part in degradation of heparin sulfate and demantan sulfate. Unfortunately, graft failure is common in MPS1 patients undergoing HSCT. One study concludes the cause of high graft failure is due to high concentration of heparan sulfate restricting stem cell migration by altering the cytokine-gradient formation (Watson H.A. et al 2014). Variable musculoskeletal disease progression was reported in a standardized follow-up study of eight children after successful stem cell transplant, including progression of scoliosis and acetabular dysplasia (Grigull L. et al, 2011). HSCT may help to slow the progression of the bone phenotype, preliminary research suggest improved prognosis for patients undergoing HSCT before musculoskeletal pathology develops.

Unfortunately, ERT and HSCT have low efficacy in treating the skeletal manifestations requiring MPS1 patients to undergo surgical intervention to combat painful bone abnormalities. A clinical study on 72 patients with MPS1 with severe thoracolumbar kyphosis argues surgery is required to combat the multifactorial trunk imbalance despite patients receiving Laronidase with orthopedic management (Genevois K.A. et al, 2013). Progression of scoliosis, gibbus formation, acetabular dysplasia, coxa valga and compression of *N. medianus* (Carpal tunnel syndrome) became more pronounced in children after receiving stem cell transplant (Grigull L. et al 2011).

Replacing surgical intervention with a new therapeutic will only be plausible if the molecular interactions leading to the bone phenotype in MPS1 are characterized.

Emerging Treatment Options. In an effort to improve growth deficiencies found in Hunters Syndrome and Hurlers Syndrome despite treatment with HSCT and ERT a recombinant form of human growth hormone was developed and clinically tested. In the clinical study evaluating the outcome of treatment with recombinant human growth hormone (rGH) revealed no significant difference in growth velocity compared to children not treated with rGH however individual response was highly variable (Polgreen L.E. et al 2009). Treatment of Hurlers Syndrome with rGH is under debate due to a concern of increased musculoskeletal pathology (Polgreen L.E et al 2009 & Hertel N.T. 2005). To enhance the current treatment options the limited knowledge of how accumulation of GAG's alters the skeletal structure must be expanded.

Skeletal Structure

Organization of the osteons are divided into two types of structural patterns, cortical bone and trabecular bone. Overall the skeletal system is comprised of approximately 80% cortical bone and 20% trabecular bone, although exact ratios are varying depending on the geometry of the specific type of bone (long, short, flat or irregular). Trabecular bone is found at the diaphysis of long bones, as well as in the pelvic bones, ribs, calvarial bone and inside vertebrae (Figure 1). Typically, vertebrae are approximately 25% cortical and 75% trabeculae and radial diaphysis of long bones are approximately 95% cortical bone and 5% trabeculae. Cortical bone is composed of cylindrical osteons collectively referred to as the Harversian system with 5% porosity

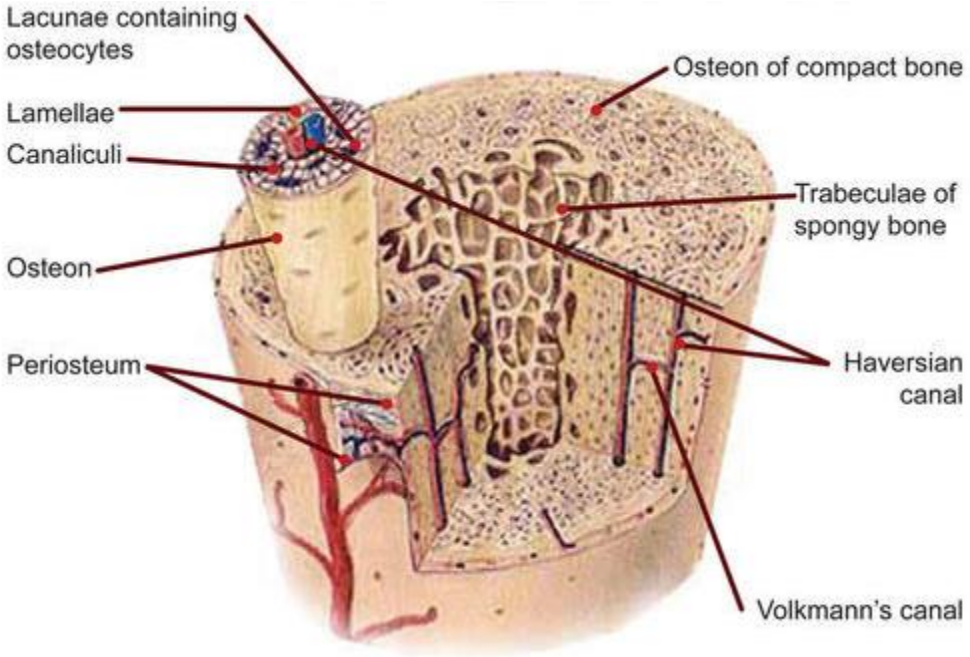

Figure 1. Skeletal Structure. Cortical bone is located around the circumference of the bone lined by the periosteum and trabeculae (spongy bone) is located inside the circumference lined by the endosteum (not labeled).

(Figure 1). Trabeculae is composed semilunar osteons, giving the appearance of plates and rods. Organic material composes approximately 25% of bone tissue with type I collagen as the major component. The 75% of inorganic material is primarily composed of a network of hydroxyapatite $[Ca_5(PO_4)OH]_2$. The collagen network is formed from collagen fibrils laid down in a lamellar pattern, this overlapping design is stronger than the disorganized pattern of woven bone.

Bone Homeostasis

The major function of the skeletal system is to provide structural support, protection of vital organs, hematopoiesis, and mineral balance. Many molecular interactions and pathways are involved in the process of regulating bone turnover to maintain the complex balance between bone formation and bone resorption**.** Bone tissue is a major storage for calcium supply, strongly linking bone homeostasis to calcium concentrations. Calcium is a major signaling molecule, and blood levels are tightly regulated. There are systematic and local factors used to regulate bone homeostasis. Systematic factors include parathyroid hormone, calcitonin, calcitriol, glucocorticoids, thyroid hormone and estrogen. When calcium concentration is high in the circulatory system, chief cells located on the parathyroid gland stimulate and increase intracellular calcium levels. The increase of calcium decreases the secretion of parathyroid hormone (PTH). This atypical response to hypercalcemia means PTH levels will increase when there are low levels of calcium. PTH directly targets bone to increase bone resorption, supplying the body with a source of calcium. PTH also directly affects kidney and indirectly affects the gastrointestinal tract to also restore circulatory calcium to basal

levels. PTH induces bone stromal cells to secrete cytokines, like interleukin-6 to stimulate bone resorption and induces osteoblasts to increase RANKL secretions and decreases OPG secretions to stimulate bone resorption. Both of these effects increases bone resorption by stimulating osteoclastogenesis. Continual elevations of PTH shifts bone homeostasis to have a net increase in bone resorption. However, when the elevation of PTH, is brief the shift will be to a net increase in bone formation because PTH also stimulates osteoblastogenesis and increases osteoblast survival. PTH increases intracellular cAMP causing a release in Insulin Growth Factor-1 (IGF-1).

With hypercalcemia conditions, calcitonin, a 32 amino acid peptide, is released from perifollicular cells on the thyroid gland. Calcitonin acts directly on osteoclasts inhibiting bone resorption activity. Glucocorticoids decrease bone formation by promoting apoptosis of osteoblasts and osteocytes. Thyroid hormone provides and overall net increase in bone turnover, which increase bone resorption more than bone formation. Estrogen also inhibits osteoclasts and has antiapoptotic effects on osteoblasts thus resulting in an overall net increase in bone formation. Calcitriol is the active form of vitamin D, [1α, 25 dihyroxy-Vitamin D]. It increases the absorption of calcium by increase the transcellular transport of calcium in the duodenum and increases the resorption go calcium in the distal tubule of the kidney. Calcitriol also increases osteoclast number and activity.

Osteocalcin, a biomarker for bone formation was found to be significantly higher in children with MPS compared to healthy children. Bone-specific alkaline phosphatase (BSAP) and urinary pyridinoline also tended to be higher in MPS children. There were several limitations to this study including limited power to find associations due to small

cohort sizes. Additionally, the different forms of MPS and specific treatment plans were not taken into consideration, which could have influenced the levels of biomarkers. Lastly, reduced physical activity seen in patients with MPS1 could be primary to influencing bone biomarkers than accumulation of GAG influence on bone biomarkers. The biomarkers were not found to have an influence on bodily pain or physical-function scores (Stevenson D.A, et al, 2014).

Basic Remodeling Unit

To maintain the integrity of bone the temporary anatomical structure called the basic remolding unit (BMU) repairs areas of bone that have sustained damage due to mechanical stress or cell aging (Figure 2). The BMU is composed of four cell types: osteoclasts, bone lining cells, osteoblasts and osteocytes. Together these four cell types preform the stages of bone remodeling: activation, resorption, reversal and formation. Osteoblasts are cuboid polarized cells responsible for laying down the collagen fibrils (Figure 2). They are derived from mesenchymal stem cells and eventually will give rise to osteocytes, bone lining cells or undergo apoptosis. Osteocytes are the main bone cell type, composing 90-95% of all bone cells. They develop from osteoblasts that became embedded in the newly formed bone matrix. Osteocytes act as mechanosensors, signaling for activation of bone remodeling. Bone lining cells (BLCs) are quiescent flat-shaped osteoblasts (Figure 2), with the ability to convert back to osteoblasts given the correct stimulus. The role of BLCs are still under investigation, but assumed roles include protecting bone from unwarranted resorption and cleaning the resorption pit to facilitate reversal (Everts V. et al, 2002). Lastly, osteoclasts are terminally differentiated

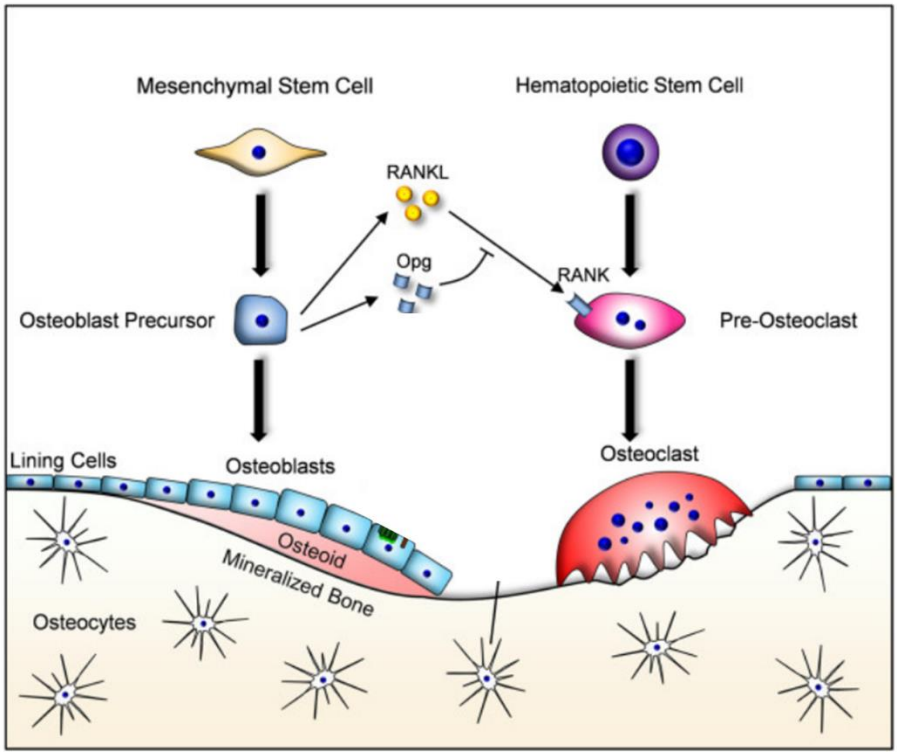

Figure 2 Bone remodeling Unit Osteoclasts are polarized bone resorbing cells derived from hematopoietic stem cells (on right). After bone resorption coupling signal pathway stimulate osteoblasts to replace the mineralized bone (on left). Osteoblast are derived from mesenchymal stem cells, osteoblasts and fibroblasts (not depicted here) secrete RANKL a ligand used to stimulate osteoclastogenesis and they secrete osteoprotegerin (OPG) a decoy receptor blocking RANKL from binding to its receptor RANK on pre-Osteoclasts. Bone lining cells cover the surface of bone and do not have a clearly defined role. Osteocytes act as mechanosensors develop from osteoblasts that become surrounded by mineralized bone (Copied from Yorgan T.A. et al 2014 with permission)

multinucleated cells derived from hematopoietic stem cells (Figure 2). They have the role of resorbing bone by secreting hydrogen protons and various proteinases. Osteoclasts also regulate the role of osteoblasts by the secretion of cytokines and help to maintain the hematopoietic stem cell niche. In mice deficient in β-glucuronidase representing MPSVII, osteoclast morphology was seen to lack the ruffled membrane and have abnormal large vacuoles (Monroy M.A. et al, 2002).

Osteoclastogenesis

Part of bone remodeling is the differentiation of hematopoietic stem cells into mature osteoclasts. Marrow stromal cells and osteoblasts secrete monoclonal stimulating factor-1 (CSF-1), Receptor Activator of Nuclear Factor κ B Ligand (RANKL) and osteoprotegerin (OPG) (Figure 2). CSF-1 is required for the survival and proliferation of osteoclast-precursors. It is also required for the survival of osteoclasts and the cytoskeletalon rearrangement needed for bone resorption. RANKL belongs to the TNF superfamily required for osteoclast maturation. RANKL binds to Receptor Activator of Nuclear Factor κ B (RANK) located on the membrane of the osteoclast by a signaling cascade not fully described, but there is an upregulation of the several transcription factors including *NFAT2* and *Fos.* Osteoprotegerin (OPG), also known as osteoclastogenesis inhibitory factor (OCIF), is a decoy receptor for RANKL, and significant levels of OPG block RANKL from activating RANK (Figure 2).

Bone Remodeling: Activation, Resorption, Reversal and Formation

Activation. Each osteocyte has approximately 50 cytosolic processes that extend out of the lacunae and into the canaliculi connecting to neighboring osteocytes via gap junctions. The gap junctions formed by connexin keep osteocytes linked metabiocally and electrically (Clarke B., 2008). Signaling molecules, such as prostaglandins and nitric oxide can move rapidly through the lacunocanalicular system. Mechanical stress in weak bone tissue, due to age or damage, will be detected within the syncytium of osteocytes. The piezoelectric effect occurs in osteocytes and is the conversion of mechanical stimuli to biochemical stimuli. Mechanical stress has been seen to regulate Interlukin-6, Interlukin-7, and TNFα (García-López et al 2013). The biochemical stimuli signals for the activation of bone remodeling. M-CSF1 and TNFα, secreted by osteoblasts will stimulate osteoclastogenesis. TNFα reduces bone formation by mature osteoblasts and increases bone resorption by osteoclasts. Treatment on fetal calvaria precursor cells with TNFα reduced the cells ability to form mineralizing nodules and decreased the skeletal specific matric proteins osteocalcin (Gilbert L. et al 2000). It was determined by northern analysis that TNFα inhibited the expression of insulin-like growth factor (IGF-I) but not bone morphogenic factors 2, 4, or 6 or skeletal LIM protein (Gilberet L et al, 2000).

Bone remodeling begins with the recruitment and activation of mononuclear monocyte-macrophage osteoclast precursors to sites of damage or weaken bone. Osteocytic apoptosis acts as a chemotactic signal for bone resorption, osteocytes have been seen to be engulfed by osteoclasts (Boabaid F. et al 2001). Multi-mononuclear cells fuse to form one multinucleated preosteoclast, which then attaches to the bone matrix by integrins binding to RGD-peptides in the matrix.

This fusion is formation of podosomes, an F-actin core surrounding by integrin and cytoskeleton proteins rich with RGD amino acids. The main connection is via the $\alpha_v\beta_3$ integrin binding to osteopontin and bone sialoprotein (Clarke B. 2008). Another connection included the intergin β_1 on the surface of an osteoclast binding to collagen, fibronectin or laminin in the bone matrix. (Florencio-Silva et al, 2015). Formation of the posodome facilitates the formation of the annular sealing zone keeping the bone resorption pit tightly sealed for proper acidification. The number of actin rings were seen to be reduced in IDUA$^{(-/-)}$ mice by 30% compared to wild-type mice (Wilson et al, 2009). In a study on MPSVIII, a related lysosomal storage disease, enzyme deficient mice were concluded to not properly form the ruffled border by GAGs interfering with attachment of osteoclasts to the bone matrix (Monroy M.N. et al, 2002).

Resorption. Polarization of osteoclasts occurs upon attachment to the bone matrix, there are four domains of an activated osteoclast: sealing zone, ruffled border, basolateral border, and the functional secretary domain (Florencio-Silva et al, 2015). Bone resorption is the dissolution of hydroxyapatite crystals and degradation of the organic matrix by secretion of protons and proteinases from the ruffled border into the bone remolding compartment (BRC). The ruffled border is a membrane domain formed by microvilli, isolated from the surrounding tissue by the sealing zone. Phase one of bone resorption is dissolution of the hydroxyapatite by acidification of the BRC. Vaculolar proton ATPase pumps located on the ruffled border transports protons into the BRC. The intense concentration of protons help to dissolve the hydroxyapatite crystals by lowering the pH to 4.5. To sustain the electrical optimal level chloride ions are pumped via the choride-ion pump CIC-7. Internal pH of the resorbing osteoclast is maintained by a

HCO_3/Cl^- exchanger located of the basolateral border. Alklation of the cells is prevented by HCO_3^- ions also being transported into the extracellular space. Chloride ions are transported into the osteoclast to sustain intracellular concentration (Mulari M. et al 2003).

Phase two of bone remodeling is the degradation of the organic matrix by exposure to proteolytic enzymes. Tartrate-resistant acid phosphatase (TRAP5b), matrix metalloproteinase-9 (MMP-9) and cathepsin K are released into the BRC. Cathepsin K is a cysteine protease that degrades collagen during acidic conditions. Levels of cathepsin K-specific cleavage sites on type II collagen was detected by an antibody and a significantly lower level of cathepsin mediated neoepitope exposure on type II collagen was found for $IDUA^{(-/-)}$ mice (Model: 129:C57BL/6) compared to wild-type mice (Wilson et al, 2009). Also heparin sulfate and demantan sulfate have been reported to inhibit the activity of Cathelpsin K (Wilson, et al 2009). Degraded material and bone resorption proteins are endocytosed by the osteoclast and transported to the secretory domain (Florencio-Silva et al, 2015). Resorption results in the formation of saucer-shaped dips called Howship's lacunae in trabecular bone and Haversian cancels in cortical bone. $IDUA^{(-/-)}$ mice (Model:129:C57BL/6) were seen to have shallower resorption pits along with a lower number of pits compared to wild-type mice (Wilson et al, 2009). Resorption is a 2-4 week process and is regulated by RANK, OPG, IL-6, IL-7, CSF-1, parathyroid hormone, 1,25 D_2 and calcitonin.

Reversal. When bone is undergoing bone remolding, there is a tight connection between bone resorption and bone formation. They are strongly coupled together. The mechanism in which resorption and formation stay tightly coupled is still under

investigation. One study suggests BLC have a role in coupling resorption to formation. After an osteoclasts leaves the how ship's canal, a bone lining cell comes and removed the remaining collagen fribils that need degrading. They release a signal for osteoblasts to come to the canal to refill it with new bone. Proposed signaling molecules facilitating the transition are TGF-β, IGF-1, IGF-2, BMP, PGDF and FGF (Clarke B, 2008). TGF-β has been seen to correlate with bone turnover and correlate with osteocalcin and BSAP levels. Another proposed mechanism of reversal includes semaphorins, cysteine-rich signaling proteins, facilitating osteoclast-osteoblast formation. Sema4D prevents bone formation during bone resorption, and Sema34 on osteoblast prevent osteoclastogenesis (Floriencio-Silva et al 2015).

Formation. Finally, the last phase of bone remolding is bone formation, which takes between 4-6 months to complete. Osteoblasts synthesize new collagenous organic matrix and regulate the mineralization of the matrix. Osteoblasts regulate the mineralization by releasing small membrane bound vesicles with a high concentration of phosphate, calcium and enzymes that destroy mineralization inhibitors. The mineral composition of bone tissue is mostly comprised of hydroxyapatite along with carbonate, magnesium, and acid phosphate. Proteins that contribute to facilitating mineral maturation are alkaline phosphate, osteocalcin, osteopontin and bone sialoprotein. There are two phases to bone matrix synthesis: vesicular phase and the fibrillar phase (Anderson H. C. 2003) Chondrocytes and osteoblasts synthesize extracellular matrix vesicles designed to allow the intravesicular concentrations of calcium and phosphate to increase. Vesicles contain sulphanated proteoglycans that immobilize calcium ions due to their negative charge and they contain that immobilize phosphates. Osteoblasts release a

protein that will degrade sulphanated proteoglycans, thus releasing the calcium ions inside the vesicles. Alkaline phosphatases will degrade phosphate containing compounds releasing the phosphate ions inside the vesicles (Yoshiko Y. et al 2007). Phosphates and calcium concentrations continue to climb forming hydroxyapatite crystals. These vesicles also have a nucleational core composed of complex proteins in order help precipitate the hydroxyapatite crystals, impurities are removed as the phosphate-calcium crystals grow. Eventually, the vesicles will releasing the hydroxyapatite crystals into the extracellular matrix. The rupture of the vesicles is followed by the collagen fribrils depositing on the hydroxypatitie crystals.

Tartrate resistant Acid Phosphatase form 5b TRAP5b

The discovery of Tartrate resistant Acid Phosphatase, also referred to as Purple acid Phosphatase, was in the 1970's, when it appeared as the most cathodic of five separate acid phosphatase bands on an acidic disc gel electrophoresis (nondenaturing polyacrylamide gel electrophoresis) (Li CT et al, 1970). Two bands appeared on the PAGE, the difference between the two bands were sialic acid residues present on the hand denoted as form 'A' of TRAP5. TRAP5a is secreted from macrophages and dendritic cells and is observed during inflammatory conditions. The second band on the gel was denoted as form 'B' of TRAP and is secreted from osteoclasts during bone remodeling. TRAP5a also has a proteasesensitivy loop-peptide not found on TRAP5b. In fact the proteolytic cleavage of the proteasesensitive loop-peptide by cysteine proteases is found to increase the activity of TRAP. In a neutral pH, TRAP acts as a generator of reactive oxidizing species (ROS), but in acidic conditions TRAP5b acts as a tyrosine

phosphatase primarily targeting the extracellular proteins attached to an aromatic ring such as osteopontin and bone sialoprotein (Kaija et al 2002).

The structural design of TRAP included two sites for N-linked oligosaccharides,a disulfide bond, an exposed protease sensitive loop peptide and a binuclear iron center with 3+ ferric ions (Hallween J. 2006). Redox-state of the 2nd iron and the disulfide bond affects the activity of TRAP. Excision of loop and binding of mannoses may also increase activity.

Vesicles containing degraded material and TRAP5b located in the resorption compartment are acidic allowing cathepsin K to cleave the loop-peptide, increasing the tyrosine phosphate activity of TRAP5b. When the vesicles move away from the resorption lacuna their pH is changed to neutral, providing an optimal environment for the ROS generating activity of TRA5b. The generation of ROS finalizes the degradation of the organic matrix components transcytosis to the functional secretory domain FSD. Degradation products and TRAP5b are released from the FSD of the osteoclast and released into the blood circulation.

Recall, osteoclasts secrete protons into the bone remodeling compartment (BRC). Numerous clinical studies have demonstrated elevated TRAP 5b levels in bone diseases such as postmenopausal osteoporosis, breast and prostate cancer bone metastases, renal bone disease, multiple myeloma, and Paget's disease of bone (Halleen J, 2006). Antiresorptive treatment efficacy studies using human *in vitro* osteoclast cultures have demonstrated that secreted TRACP 5b activity correlates significantly with both osteoclast number and bone resorption (Hallween J. 2006).

Serum TRAP5b have been seen to be a reliable indicator of bone resorption, correlating significantly with bone mineral density and other known markers of bone remodeling: bone alkaline phosphatase (BAP), osteocalcin, parathyroid hormone (PTH), and PINP (Shidara K et al 2008). Problems associated with using TRAP5b as a biomarker of bone resorption includes high diurnal variability, effects of feeding and renal function on the values obtained caused by the gastrointestinal hormone glucagon-like peptide-2 (GLP-2). Also, TRAP5b is suggested to rapidly lose its activity from freeze-thawing cycles (Hallween J, et al 2005).

Procollagen Type I N-terminal Propeptide (PINP)

Type I Collagen is the most abundant protein found in bone composing approximately 90% of the extracellular matrix. It is derived from procollagen type I secreted by osteoblasts and fibroblasts. Biosynthesis in the fibroblasts occurs to produce fibroproliferative responses and in the osteoblasts for formation of the bone matrix. Type I collagen consists of a triple helical molecule formed from two α1 (I) chains and one α2(I) chain. It. In order to keep type I collagen from spontaneously aggregating into fibrils, it is secreted as larger precursor procollagen protein with large propeptides domains at the amino and carboxyl ends (Figure 3).

Type I procollagen consists of the same structure as Type I collagen, a triple helical molecule formed from two pro-α1 (I) chains and one pro-α2(I) chain non-covalently link together (L.V. Hale et al. 2006). Procollagen triple helix is flanked by nonhelical telopeptides and N-terminal (PINP) and C-terminal (PICP) propeptides. The pro-α2(I)

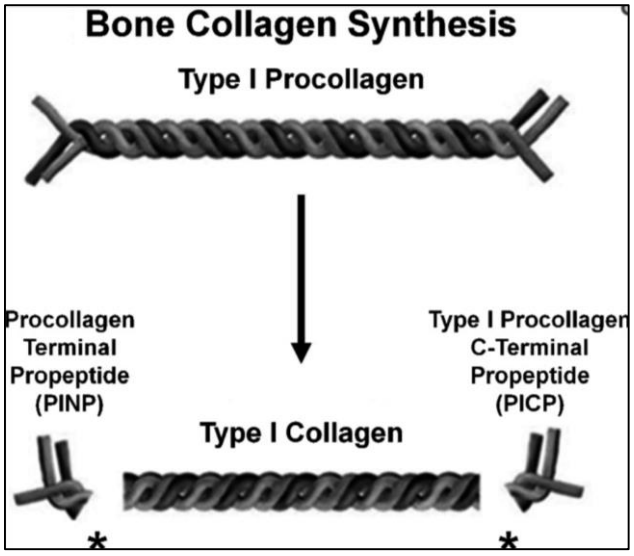

Figure 3. Bone Collagen Synthesis. New mineralized bone formation begins by osteoblast secreting type I procollagen. Mature type I collagen is formed after the cleavage of the globular propeptides, Procollagen Terminal Propeptide (PINP) and Type I Procollagen C-terminal Propeptide (PICP). (Figure copied from Krege J.H. et al, 2014)

chain lacks the N-terminal domain. The amino domain is smaller and rod-like and the carboxyl end is globular-like. The post-translation cleavage of the carboxyl end is required before the assembly of the fibrils can begin but the amino end can remain on as the fibril becomes thicker. Endoproteases cleaved PINP and PICP from the triple helix to yield Type I collagen and circulating PINP and PICP in the extracellular space. This newly formed Type one collagen is where hydroxypatite crystals mineralize to form new bone. Serum PINP concentrations are directly proportional to synthesis of type I collagen and bone formation.

Serum PINP concentrations are a reliable indicator of bone formation, measurement of serum PINP concentration is supported by the International Osteoporosis Foundation, the International Federation of Clinical Chemistry and Laboratory Medicine and the National Bone Health Alliance as the most accurate biomarker for bone formation (Bauer D. et al 2012). PINP has been demonstrated as viable early serum biomarker in the rat for assessing bone anabolic activity. After weekly subcutaneous injections of PTH (1-38), a bone anabolic agent, PINP concentrations were seen to increase followed by an increase in bone mineral density (Hale L.V. et al 2007).After being released from type one procollagen, PINP is release into circulation for disposal. A radioactive-label pulse-chase study demonstrated the major uptake for PINP in rats was the liver, 78% of PINP radioactivity was recovered in isolated endothelial chief cells, 21% in parenchymal cells and 1% in Kupffer cells. These findings indicate the clearance of PINP is a majority physiological function of the scavenger receptors on endothelial chief cells (Melkko et al. 1994).

When evaluating levels of bone formation, it is important to distinguish between the intact trimeric form of PINP and the small antigenic form of PINP. The small antigenic form is also referred to as the monomeric form. The trimeric form of PINP is the result of bone formation. The small antigenic form of PINP could originate from several sources including type one pN-collagens in the soft tissue and Type III pN-collagen found in wound healing. Serum small antigen PINP could also be due to heat denaturation causing the dissociation with the trimeric form however this was seen to be unlikely. When referring to both forms (total concentration) the abbreviation is P1NP.

Both the trimeric form and antigenic form can be found in circulation therefore both are located in blood serum samples used for research purposes. If an assay tests for total PINP the concentration of both forms will be measured. Thus intact PINP levels could seem to be elevated resulting in incorrectly analyzing increased bone formation. Assays used to analyze bone formation should only test for intact PINP. The total P1NP assays measures both trimeric and monomeric forms of while the intact PINP measures only the trimeric form (Koivula et al. 2010).

The larger antigen is the trimeric propeptide representing the intact PINP and the smaller antigen contains only a single proa1-chain representing the monomeric form. The total molecular weight of trimeric propeptide is about 35,000kDa and its constituent chains 14,250KDa (proa1-chain) and 5500KDa (proa2-chain). In a study combining data from thermal transition, SDS-PAGE, and mass spectrometry indicate the high-molecular weight form of PINP represents the unstable trimeric structure. Additionally, the low-molecular weight form represents the monomeric α1 chain released from the trimeric structure by heat (Brandt et al, 1999). Later, it was determine heat denaturation from

trimeric PINP was not a source of the small antigen form. Due to PIIINP, derive from collagen Type III, resulted in an increase of the small antigen form despite the fact Type III collagen is held together by sulfide bonds that are unbreakable by heat. From this study, it can be assumed the small antigen form must have another source beside heat denaturation of the trimeric form.

Intact PINP is taken up rapidly by the liver. The monomeric or antigen form is dependent for clearance by the kidney (Koivular et al 2012). Renal insufficiency increases the concentration of the smaller antigen from of PINP influencing the total concentration of PINP seen in the assay. Other causes of increased concentration of the small antigen include chronic immobility, and breast cancer with metastases. . In Finnish blood samples patients with chronic kidney failure had a significantly higher amount of the monomeric form of PINP before heamdylasis. (Koivula et al 2010). PINP is liberated from procollagen before mineralization therefore there is no PINP in mineralized bone. It should be noted there is no evidence PINP would still be antigenically active when released from the liver after degradation.

Mouse Model

Improvement of enzyme replacement therapy and development of novel treatments for MPS I was ameliorated by the generation of murine models deficient in IDUA. One of the first animal models, was generated by targeting disruption of the IDUA locus by insertion of a neomycin resistance cassette using a restriction enzyme site on exon VI. No detectable IDUA activity was reported for this murine model along with increased GAG excretion and bone abnormalities. As early as three weeks, flattened

facial features and thickening of digits was reported with continual progression of dysostosis up to 15 weeks of age. Lysosomal storage was reported to increase in several cell types including Kupffer cells, Glial cells, reticuloendothelial cells and splenic sinusoidal lining at four weeks of age; and hepatocytes, neurons, chondrocytes and renal tubular cells at eight weeks of age (Clarke L.A. et al, 1997).

Further characterization of this murine model reported serve dysostosis multiplex and progressive neuronal degradation. Radiographic examination revealed thickening of the diaphysis of long bones and widening of the malar processes and zygomatic arch. In addition, bone histopathology revealed abnormalities in the development of the growth plate and –D-abnormalities on the structure of the cortical bone (L.A.Clarke et al. 1997).

One weakness of the murine model described above is the nonspecific disruption the *IDUA* locus on exon VI, eliminating the ability to test treatment regimens on specific mutations. With the potential of of gene therapy for treatment, it is important to have small animal models with mutations analogous to human mutations in IDUA. Thus, another small animal model was generated using gene replacement methodology with a neomycin resistance cassette (Figure 4A). The replacement targeting construct contained the IDUAW392X nonsense mutation which is analogous to the *IDUA W402X* mutation the most common human mutation in patients with MPS I. The codon TGG was replaced with TAG resulting in premature termination in translation. Characterization of IDUA activity and GAG accumulation confirmed the mouse model exhibited similar phenotypic features as patients with MPS I (Wang D. et al, 2009).

The replacement targeting construct was composed of the *IDUA* exons 3-14 from 129/SV mouse genomic DNA with the IDUA-W392X mutation (Figure 4), neomycin

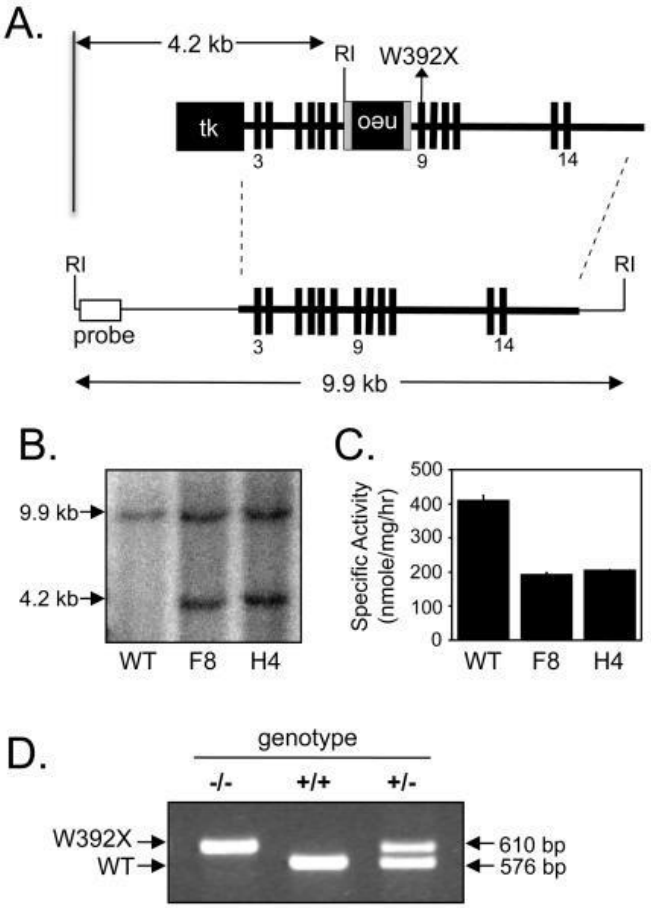

Figure 4. Generation of the Mouse Model *A)* replacement targeting construct contained the *IDUAW392X* non-sense mutation and the gene for neomincin resistance *B)* EcoRI digest *C*) Specivty activity of IDUA in wild-type mice and two linage of *IDUAW392X*. *D)* Agarose Gel Electrophoresis of isolate IDUA sequence, Wild-type allele is 576bp and mutated allele is 610bp. (copied from Wang et al, 2009, with copyright permission)

resistance positive selective marker and thymidine kinase negative selective marker (Figure 4A). The 129/SV embryonic cells were electroporated with the targeting construct and successfully integrated cell clones were placed in C57BL mouse blastocysts. Integration was confirmed by Southern Blotting preceded by an EcoRI digest results in a 4.2 kb fragment for the mutated IDUA allele and a 9.9kb fragment for the wild-type allele (Figure 4B). The removal of the neomycin resistance cassette by mediated recombination left behind a 34bp fragment in an intron of the mutated IDUA providing a useful mechanism for genotyping (Figure 4D). The mutated *IDUA* allele results in a 610bp fragment and the wild type IDUA allele results in a 576bp fragment by PCR and gel electrophoresis (Wang D. et al, 2009). Biochemical characterization analysis of the IDUAW392X murine model reported the IDUA activity of liver and brain tissue samples were below the detection level in IDUA-deficient mice. Heterozygous mice were reported to have approximately 50% IDUA activity compared to wild-type levels. Analysis of GAGs reported an increased in urine excretion and tissue accumulation. Also, levels of *IDUA* mRNA transcripts were reduced in IDUAW392X mice by 30% to 50% compared to wild-type mice (Figure 4C). Histological analysis revealed increased lysosomal storage in Purkinje cells in the cerebellum and neurons in the medulla. Lysosomal aberrations were also confirmed by electron microscopy revealing foamy macrophages and increased vacuolation in IDUAW392X mice. In addition, activity of other lysosomal enzymes, β-D-glucuronidase and β-D-hexosaminidase, were reported to have increased in Idua-W392X which is thought to be compensation for the loss of IDUA. Finally, characterization of bone parameters were reported for the IDUAW392X

murine model, revealing thickening of the zygomatic arch and progressive widening of the femur between 15 weeks of age to 35 weeks of age (Wang D. et al, 2009).

Skeletal Phenotype: Characterization of Bone Geometry and Mineral Properties

Currently, how accumulation of GAGs leads to the skeletal phenotype in MPS1 is unknown. Previous work by collaborators reported the macroarchitecture and microarchitecture structure are altered in IDUA $^{(-/-)}$ mice, along with altered physiochemical composition and percentage of porosity. Specifically, IDUA $^{(-/-)}$ mice were concluded to have increased femoral cortical thickness, increased bone marrow width and decreased femoral length. These macroarchitecture structure changes could be source of overall increased in bone strength. However, mineral composition findings suggested IDUA $^{(-/-)}$ mice may have weaker bones (Oestreich A.K. et al, 2015).

Tibial microarchitecture. Tibial microarchitecture was analyzed using microcomputed tomography (μCT) and compared between wild-type, heterozygous, and IDUA $^{(-/-)}$ mice. Cortical thickness, trabecular number, and connectivity density significantly increased in female IDUA $^{(-/-)}$ mice and cortical thickness was significantly increased in male IDUA $^{(-/-)}$ mice compared to wild-type mice. Trabecular separation significantly decrease in female IDUA $^{(-/-)}$ mice. Despite only cortical thickness increasing significant in males, other male microarchitecture properties showed similar trends as the female IDUA $^{(-/-)}$ mice (Oestreich A.K. et al, 2015).

Bone Mineral Density Distribution and Porosity. Quantitative backscattered electron scanning was used to analyze bone mineral density distribution (BMDD) and porosity using the calcium content in relation to atomic number (Figure 5). Wild-type

mice and IDUA$^{(-/-)}$ mice were determined have equivalent BMDD at the mid-diaphysis of the tibia. Also, IDUA$^{(-/-)}$ mice were seen to have a 50% increase in porosity compared to wild-type mice (Oestreich A.K. et al, 2015).

Material and Physiochemical Properties. Raman Spectroscopy was utilized to examine tibial mineral and matrix composition by quantifying the carbonate/phosphate ratio (CH_3^{2-}/PO_4^{3-}), mineral/matrix ratio (PO_4^{3-}/CH_2) and mineral/collagen ratio (PO_4^{3-}/amide I) (Figure 6). Area of hydroxyapatite is assumed to equal to PO_4^{3-} levels. No change mineral compositions were reported between male wildtype mice, heterozygous and IDUA $^{(-/-)}$ mice. Differences identified for female IDUA$^{(-/-)}$ mice were an increase in the carbonate/phosphate ratio along with decreases in the mineral/bone matrix ratio and mineral/collagen ratio in IDUA$^{(-/-)}$ mice. Although the decrease in mineral/collagen ratio did not research significance (Oestreich A.K. et al, 2015). The increase of carbonate as a substitute for phosphate was suggested to be an indication of more mature bone matrix. It is unclear if there is a decreased in mineral or increase in collagen altering the other ratios measured. The altered physiochemical properties could account for the decreased strength suggested the biomechanical integrity properties tensile strength and shear modulus of elasticity.

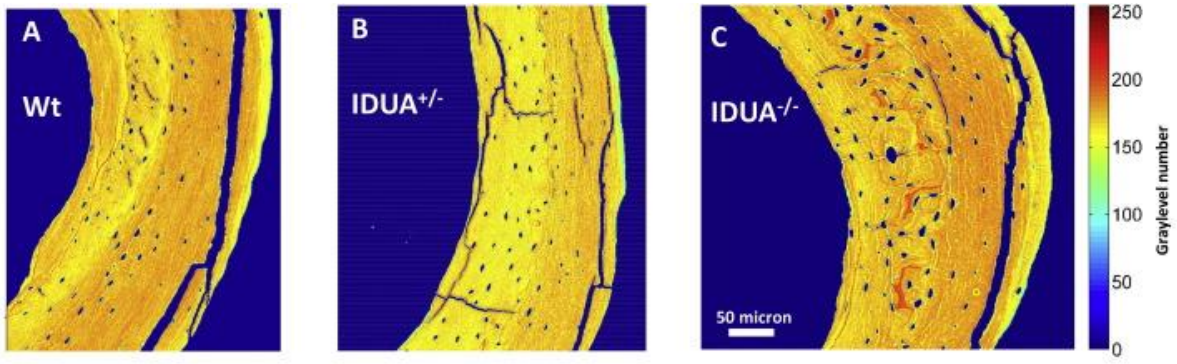

Figure 5. Bone mineral density distribution (BMDD) and porosity analysis as determined by scanning electron microscopy. Representative segments of female A) Wt, B) IDUA+/− ,and C) IDUA− /− cross-sectional BMDD images of the medial section of the mid-diaphysis of the tibia (range of 256 graylevel numbers, with red representing the greatest density of calcium and blue the least).For each sample the whole cross-sectional image was used to determine the BMDD histogram. (Copied from Oestreich A.K. et al, 2015 with permission)

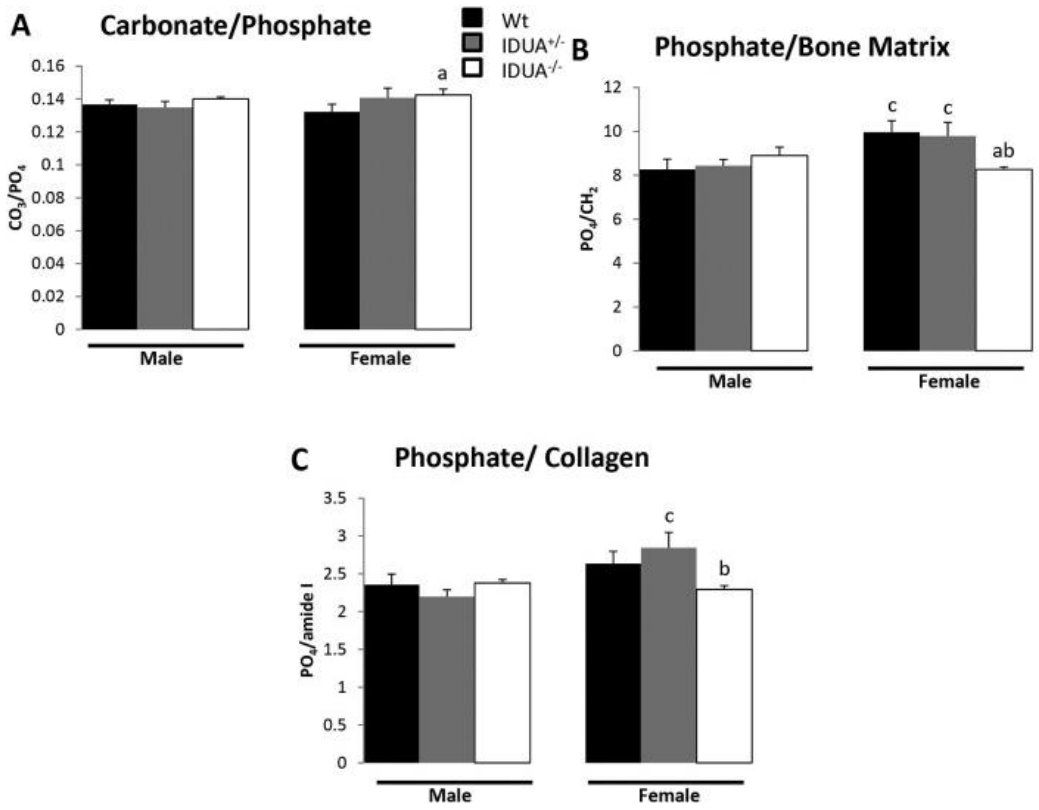

Figure 6. Physiochemical composition of the tibial cortical bone was determined using Raman spectroscopy.A) Carbonate/phosphate ratios[(CO_3^{2-} /PO_4^{3-}); indication of carbonate substitution of phosphate in the crystal lattice] were increased in tibiae from $IDUA^{-/-}$ females (white bar) compared to Wt (black bar). B) Phosphate to bone matrix ratios [(PO_4^{3-} /CH_2); indication of the relative amount of mineral phosphate to organic matrix] was decreased in tibiae from $IDUA^{-/-}$ females compared to Wt and $IDUA^{+/-}$ (graybar) littermates of the same sex. C) Phosphate to collagen ratios [(PO_4^{3-} /amide I); indication of the relative amount of phosphate mineral to collagen] was decreased in tibiae from female $IDUA^{-/-}$ compared to $IDUA^{+/-}$ littermates and had a decreased trend compared to sex-matched Wt littermates (p= 0.06). Values are means ± SE. ap ≤ 0.05 compared to sex-matched Wt,bp ≤ 0.05comparedtosex-matchedIDUA+/− ,cp ≤ 0.05 compared to genotype-matched male. Male Wt (n = 5),$IDUA^{+/-}$ (n = 5),and $IDUA^{-/-}$ (n = 4); Female Wt (n = 5), IDUA+/− (n = 4), and $IDUA^{-/-}$ (n = 5). (Copied from Oestreich A.K. et al, 2015 with permission)

Femoral Geometry and Biomechanical Strength. Femoral length was found to be reduced in IDUA $^{(-/-)}$ mice compared to wild-type and heterozygous females by µCT analysis. As well as, increased midshaft marrow diameter and increased cortical bone width. Torsional strength is described as the maximum stress a material can withstand before failing under torsion while energy loading to failure is the amount of energy absorbed by the material before rupture. Both male and female IDUA $^{(-/-)}$ mice were reported to have increased torsional ultimate strength and increased energy loading to failure (Figure 7A-C). Tensile strength is defined as max stress a material can endure before failing while force is applied at both ends in opposite directions. Female IDUA $^{(-/-)}$ mice were observed to have significantly decreased tensile strength and male IDUA$^{(-/-)}$ mice were observed to have decrease tensile strength however it did not reach statistical significance (Figure 7D). Notably, torsional strength and tensile strength exhibited opposite affects for bone strength of IDUA $^{(-/-)}$ mice. Torsional stiffness is the ratio of applied torsion to the angle of the force, there was no difference seen between genotypes for torsional stiffness (Figure 7E). There was a significant different for shear module of elasticity (Figure 7F). Elastic modulus is an intensive property of the material and stiffness is an extensive property of the structure. Overall the adverse changes in the material and physiochemical properties in bone strength are compensation by the changes to microarchitecture and geometry.

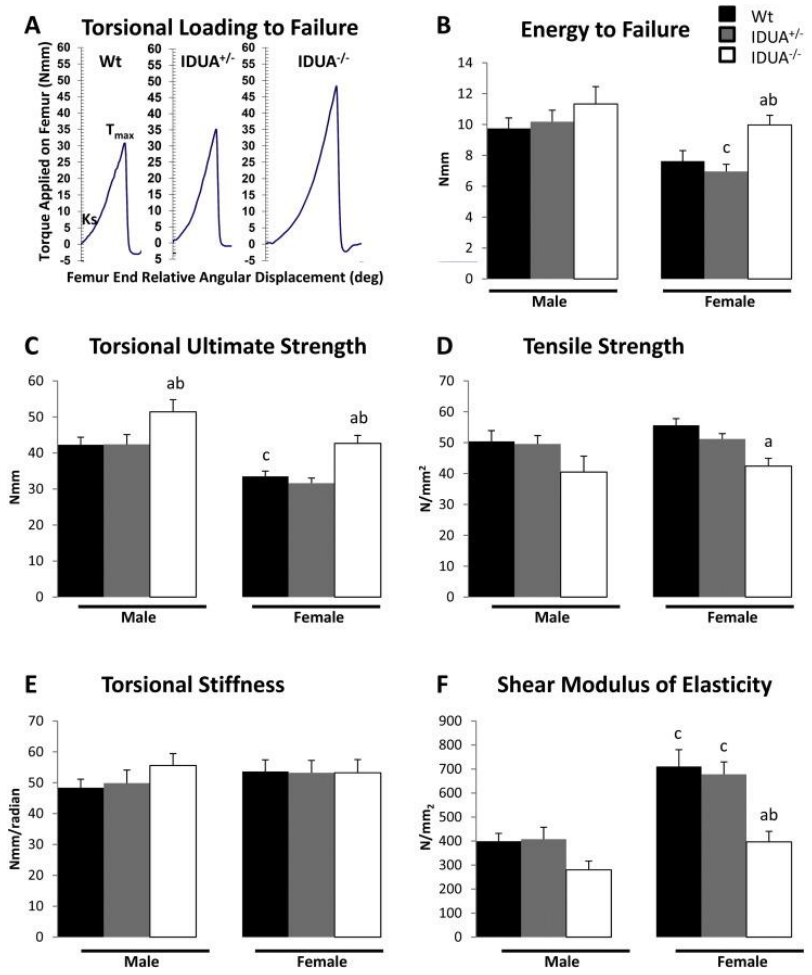

Figure. 7. Bone biomechanical integrity. A) Representative torsional loading to failure graphs from female Wt (black bar), IDUA$^{+/-}$ (gray bar),and IDUA$^{-/-}$ (white bar) femora.B) Energy to failure (U; the amount of energy the bone can absorb prior to fracture as measured by the area under the torque: angular displacement graph) of female IDUA$^{-/-}$ femora is increased compared to sex-matched Wt and IDUA$^{+/-}$ littermates. C) Torsional ultimate failure (Tmax; the force at failure as measured by the peak of the torque: angular displacement curve) was increase in both male and female femora from IDUA$^{-/-}$ compared to sex-matched Wt and IDUA$^{+/-}$ littermates. D) Tensile strength (Su;the strength of the bone material as measured by subtracting the estimated strength contribution of the geometry component from the Tmax) is decreased in femora from female IDUA$^{-/-}$ compared to sex-matched Wt littermates. E) Torsional stiffness (Ks;the stiffness of the bone as measured by the slope of the torque: angular displacement curve between 5 and 10 Nmm) is equivalent among all genotypes assessed. F) Shear modulus of elasticity (G; an estimate of the elasticity of the bone material as measured by the Ks—the estimated contribution of the geometry component) is reduced in femora from female IDUA$^{-/-}$ compared to sex-matched WT and IDUA$^{+/-}$ littermates.ap ≤0.05 compared to sex-matched Wt,bp ≤0.05compared to sex-matched IDUA$^{+/-}$,cp ≤0.05 compared to genotype-matched male. Male Wt (n= 8), IDUA$^{+/-}$ (n= 6), and IDUA$^{-/-}$ (n= 7); Female Wt (n= 8), IDUA$^{+/-}$ (n= 8), and IDUA$^{-/-}$ (n= 5). (Copied from Oestreich A.K. et al, 2015)

Skeletal Phenotype: Characterization of Bone Remodeling Biomarkers

It is the goal of this work to help elucidate the cause of the bone phenotype seen in MPS I by analyzing bone remodeling. Skeletal biomarkers of bone formation and bone resorption will be compared in wild-type, heterozygous, and IDUA $^{(-/-)}$ mice.

To investigate osteoblast activity, levels of the bone formation marker PINP were evaluated in wild type, heterozygous, and IDUA$^{(-/-)}$ mice. Levels of osteoclast activity were investigated by determining levels of serum TRAP5b a marker for bone resorption. PINP is strongly influenced by circadian rhythm and food intake so samples should be collected during the morning fasting state do decrease variance TRAP5b is secreted exclusively from bone-resorbing osteoclasts providing a reliable tool for measuring osteoclast activity. Potential differences in serum PINP or serum TRAP5b concentrations could contribute to the increased cortical thickness and bone marrow width seen in the skeletal phenotype previously found in mice with an IDUA deficiency.

Lastly to further investigate bone turnover levels, transcription of the several biomarkers for bone metabolism were quantitated by measuring the mRNA levels of: alpha chain I and alpha chain 2 of type one collagen, RANK, OPG, TNF-α, and CSF-1 in the tibiae of wild type, heterozygous, and IDUA$^{(-/-)}$ mice. Collagen is the most abundant protein in bone, it is important to determine if a deficiency in IDUA alters the levels of two types of alpha chains of type one collagen. Since type one collagen is the main component of the organic extracellular matrix discrepancies of type one collagen transcription levels can indicate if bone formation levels are altered between the genotypes.

Decreases in RANK and CSF-1 or increases in OPG may decrease osteoclastogenesis causing a decrease in osteoclast activity. TNFα stimulates osteoclastogenesis via RANK/RANKL independent and RANK/RANKL dependent pathways, evaluating mRNA levels for TNFα could help determine in levels of bone resorption are altered in mice with IDUA deficiency compare to wild-type mice.

EVALUATION OF BONE RESORPTION BY COMPARING LEVELS OF TRAP5b

Materials and Methods

To compare osteoclast activity by genotype, the levels of Tartrate Resistant Acid Phosphatase form 5b (TRAP5b) were measured using Enzyme Linked Immunosorbent Assay (ELISA) from Immunodiagnostic Systems (IDS Code# IS-4000). In this technique concentraion of TRAP5b are measured by direct correlation with the absorbance of a substrate. Each well is coated with a primary antibody that will bind to TRAP5b which is present in the sample. The blood serum samples collected from the IDUAW392X linage are allowed sufficient time to bind to the primary antibody. A secondary antibody is washed over the plate and binds to TRAP5b. The technique is referred to as a sandwich ELISA due to the target being bound to an antibody on either side. A third antibody is then washed over the plate, this antibody is attached to a substrate. When a stop solution is washed over the plate, the substrate becomes fluorescent. The absorbance (405nm) is measured for each well and the level of TRAP5b can be calculated using the standard curve generated from the calibrators (provided in the IDS kit).

Blood serum samples were received from collaborators, Dr. Charlotte Phillp's lab at the University of Missouri. All samples were stored at -80°C until TRAP5b measurement and thawed on ice before transferred in 96 well plate. Anti-mouse antibody was reconstituted by adding 10.5 ml of Millipore water, inverted and let to incubate at room temperature for 15 minutes. The reconstituted anti-mouse antibody (100 µl) was added into all wells and incubated on a shaker for an hour at room temperature. Calibrators 0-4 and the control were reconstituted with 0.5 ml of Millipore water, mixed by inversion and incubated at room temperature for 15 minutes. The antibody coated

plate was manually washed four time by adding 250 µl of Wash Buffer to remove excess anti-mouse antibody. Calibrators and the control (100µl of each) were loaded into wells, wash buffer was not added to calibrator or control wells. Serum samples (25 µl) were added to wells containing 75 µl of the 0.9% Sodium Chloride Dilution Solution. Releasing Reagent (25 µl) was added to all wells.

The plate was incubated at room temperature for one hour while slowly shaking. The substrate solution was prepared by dissolving the substrate tablet into 5 ml of substrate buffer as directed by the kit. The wash step was repeated as done previously. Fresh substrate solution (100µl) was added into all wells. The plate was sealed and incubated at 37˚C for 2 hours. Stop solution (25µl of 0.32M Sodium hydroxide solution) was added to all wells. The absorbance of all wells was read at 405nm using a SpectraMax Paradigm Multi-Mode Detection Platform platereader.

Calibrators were run in duplicate on every plate, absorbance was averaged and used to generate the calibration curve. The calibration curve was created by plotting the Log of the average absorbance versus the Log of the calibrator's concentration. The concentrations of the calibrators and the control range were provided by the IDS kit. The calibration curve was verified by ensuring that the absorbance of the control generate a concentration within the provided range. One-way ANOVA statistical tests were used to evaluate the effect genotype had on TRAP5b concentrations (SAS Program GLM for Unbalanced ANOVA).

Results

One-Way ANOVA (GLM procedure) reported no statistical difference in TRAP5b concentrations between the genotypes (*F= 1.33, PR 0.2736*) The mean concentration for TRAP5b for male wildtype animals was 5.00 U/L (*SD=2.53, n=7*) (Table 2). The mean TRAP5b concentration for male heterozygous animals was 3.62 U/L (*SD=0.868, n=12*) and the mean TRAP5b concentration for male $IDUA^{(-/-)}$ mice was 4.581 U/L (*SD= 2.031, n=7*). (Table 2). The mean concentrations for female wildtype mice was 5.676 U/L *(SD= 2.571, n=7).* (Table 2). The mean concentration for female heterozygous mice was 4.583 U/L *(SD= 1.464, n=6*) (Table 2) and for female $IDUA^{(-/-)}$ mice was 4.029µg/L *(SD=0.1.311, n=5*) (Table 2). One-way ANOVA (GLM procedure) found no significant difference for the mean concentrations of TRAP5b between the genotypes for males and females, (males; *F= 2.28, p= 0.1162*) and (Females; *F= 1.77, p=0.1833*).

Bartlett's test of homogeneity for Variance reported the statistical difference should be evaluated using Log of TRAP5b; (TRAP5b; *PR= 0.0391),* (LogTRAP5b; *PR= 0.2889*) (Table 2). One-way ANOVA showed no statistical difference for the Log concentration of TRAP5b between genotypes (*F=0.12, PR= 0.4212*) (Figure 8).

Discussion and Conclusion

During bone resorption, vesicles containing TRAP5b are released from the ruffled border domain of a polarized osteoclast into the acidic bone remodeling compartment (BRC). TRAP5b helps to degrade the organic matrix thru tyrosine phosphatase activity. Degraded material leaves the BRC and is directly absorbed by the extracellular matrix underneath the sealing zone or the degraded material is transported to the functional

Table 2. Means and standard deviations for TRAP5b concentration (U/L) and Log TRAP5

		TRAP5b		Log TRAP5b		
Sex	Genotype	MEAN (U/L)	Std Dev	MEAN Log (U/L)	Std Dev	n
Male	WT	5.007	2.528	0.648	0.234	7
	HET	3.623	0.868	0.547	0.105	12
	IDUA$^{(-/-)}$	4.811	2.031	0.653	0.164	7
Female	WT	5.676	2.571	0.712	0.211	7
	HET	4.583	1.464	0.640	0.15328	6
	IDUA$^{(-/-)}$	4.029	1.311	0.589	0.126	5

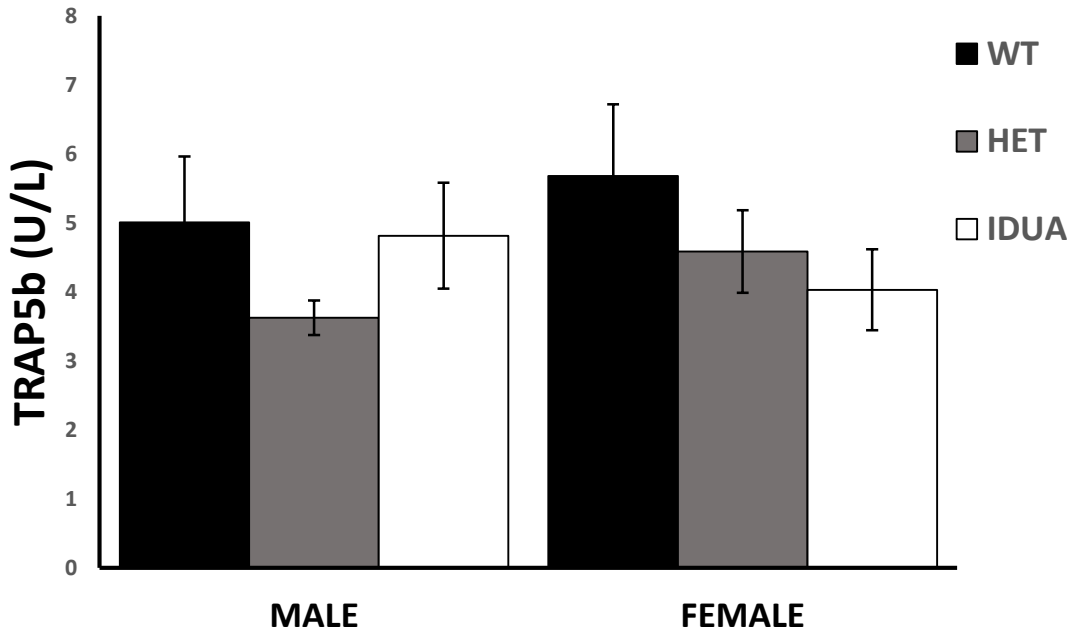

Figure. 8. Levels of Tartrate Resistant Phosphatase Form 5B (TRAP5b). Levels determined by Enzyme Link Immunosorbent Assay (ELISA) to evaluate bone resorption in Wild-type (Wt), Heterozygous HET) and IDUA$^{(-/-)}$ mice. Male Wt (*n= 7*), HET *(n= 12*), IDUA$^{(-/-)}$ (*n= 7*); Female Wt (n= 7), HET (n= 6), and IDUA$^{(-/-)}$ (n= 7). One-way ANOVA (GLM procedure) reported no significant difference for the mean concentrations of TRAP5b between the genotypes *(F= 1.33, p= 0.2736*). Bartlett's test of homogeneity for Variance (Pr > F 0.0391) reported the statistical difference should be evaluated using Log phase of TRAP5b. One-way ANOVA showed no statistical difference for the Log concentration of TRAP5b (*F=0.12, p= 0.4212*).

secretory domain (FSD) of the osteoclast by intracellular vesicular trafficking. As the vesicles move away from the resorption lacuna to the FSD their pH increases to a neutral level, providing the optimal environment for the reactive oxidizing species (ROS) generating activity of TRAP5b. This capability of ROS activity of TRAP5b has been proposed to indicate TRAP5b helps to further degrade the remaining collagen fragments inside the intercellular vesicles by producing hydroxyl radicals (Kaija H et al 2002 & Vääräniemi J et al 2004).

Unexpectedly, TRAP5b concentrations were not seen to be significantly different between wild-type, heterozygous, and IDUA$^{(-/-)}$ mice even though the IDUAW392X mouse model was demonstrated to have increased cortical width and bone marrow diameter (Figure 8). It is reasonable to assume changes in the balance of bone remolding contribute at some level to the changes in bone phenotype seen in IDUA$^{(-/-)}$ mice compared to wildtype. TRAP5b has been observed to be a reliable marker of bone resorption yet no changes were seem in TRAP5b concentration to support the hypothesis of altered levels of bone remodeling. Either levels of bone resorption are not affected by accumulation of GAGs, enzymes other than TRAP5b are involved, or the effect of GAGs accumulation has on bone resorption is mediated by another mechanism.

Raman spectroscopy and μCT reported equivalent cortical density in wildtype mice and IDUAW392X mice (Figure 6). There is a possibility that the accumulation of heparin sulfate (HS) and dermatan sulfate (DS) does not alter levels of osteoclast activity. However this seems unlikely due to the change in bone phenotype. It is also seems unlikely the copious amount of DS and HS would not have some effect on the dynamics between osteoblasts, osteocytes, bone lining cells and osteoclasts.

It has yet to be determined if TRAP5b is an adequate indicator of osteoclast activity or osteoclast number. TRAP5b activity has been proposed to remain at constant levels regardless of level of bone resorption as TRAP5b is cleaved and excytosed at the same rate in resorbing and nonresorbing osteoclasts (Hallween J. 2006). However other sources conclude TRAP5b is an indicator of osteoclast activity. Regardless of TRAP5 levels indicating osteoclast number or osteoclast activity TRAP5b can provide insight on the levels of bone resorption.

Ultrastructural analysis revealed abnormal osteoclastic morphology in a Mucopolysaccharidosis type VII (MPS VII) mouse model. A similar inherited lysosomal storage disease caused by a deficiency in β-glucuronidase (Monroy M.A et al 2002). Osteoclasts failed to form ruffled border membranes and many appeared to be detached from the bone surface. Proper attachment of the osteoclast by the sealing zone domain is important for proper degradation of the hydroxyapatite and organic matrix. In fact Monroy M.A. et al observed significantly smaller and fewer resorption pits formed by osteoclasts derived from the β-glucuronidase deficient mice compared to osteoclasts derived from normal mice (2002).

It is not unexpected for TRAP5b serum concentration to be unaltered in $IDUA^{-}$ W392X mice if TRAP5b is an indicator for number of osteo85s as opposed to indicating osteoclast activity. Bone resorption could be lower in $IDUA^{(-/-)}$ mice without effecting the level of osteoclast number. Bone resorption could still be decreased if osteoclasts are unable to form tight attachment to the bone matrix due to the accumulation of heparin sulfate (HS) and dermatan sulfate (DS).

If TRAP5b is an indicator of osteoclast number, serum concentration of TRAP5b could be altered if there was an increased in osteoclastogenesis. To evaluate the levels of osteoclastogenesis the expression levels of M-CSf-1, RANK and OPG were evaluated in the next part of the study by comparative qPCR.

EVALUATION OF BONE FORMATION BY COMPARING LEVELS OF PROCOLLAGEN TYPE I N-TERMINAL PROPEPTIDE (PINP)

Materials and Methods

Enzymeimmunioassy (EIA) kits (Cat# SB-TR201A) purchased from IDS (Immunodiagnostics Systems) were used to measure the trimeric, intact form of PINP in serum from wildtype, heterozygous and IDUA$^{(-/-)}$ mice. The assay is specific for measuring bone formation as it does not measure the total concentration (P1NP) by including the small antigen form. EIA, a competitive assay was used in place of the traditional "sandwich" enzyme-linked immunosorbent assays ELISA technique due to the small size of PINP. Steric hindrance prevents two antibodies binding to PINP at the same time. The EIA kits were stored at 4°C until use.

Blood serum samples were received from collaborators, Dr. Charlotte Phillp's lab at the University of Missouri. All samples were stored at -80°C until PINP measurement and thawed on ice before transferred in 96 well plate. All Calibrators (0-4) and controls (1-2) were reconstituted with 5ml of Millipore water, biotin was reconstituted with 8ml of Millipore water and all were left at room temperature for 15 minutes. Remaining calibrators and controls were stored 4°C between trials and remaining biotin was stored at 4°C between trials. The concentrated wash solution was added to 950ml of Millipore water and stored at room temperature.

Calibrators and controls were added (50µl) to appropriate wells on a standard clear 96well microtiter plate. Serum sample were added in triplicate at 5µl per well followed by 45 µl of sample diluent. All samples were added within 15minutes of each

other as directed by the kit. Sample numbers included 292, 307, 308, 311, 313, 331, 341, 354, 355, 359, 364-369, 375, 376, 379, 380-382, 401, 402, 404, 406, 407, 409, and 410. Samples are allowed to bind to the primary antibody attached to the bottom of the wells. The PINP-biotin was added (50µl) to calibrators, controls and sample wells, and any primary antibody not bound to PINP will bind to the PINP-Biotin complex. The plate was covered with an adhesive plate sealer and incubated at room temperature for 60 minutes shaking at 500 to 700rpm. Each well was washed three times with 250µl of Wash solution.

Enzyme conjugate (150µl) was added to all wells, this secondary antibody binds to the PINP-Biotin. The plate was covered and incubated at room temperature for 30 minutes followed by a repeat of the three wash steps. The color substrate, Tetramethylbenzidine (TMP), was added (150µl) to all wells and will bind to the enzyme conjugate. TMP was added in the dark due to risk of degradation when exposed to ultra violet light. The plate was covered and incubated in the dark for 30 minutes at room temperature. Hydrochloric acid was added (50µl) was added to stop the reaction. Optical densities (OD) were recorded at 450nm and 652nm with SpectraMax Paradigm Multi-Mode Detection Platform. In a pH neutral environment TMB exists as a pale blue charge-transfer complex of the parent dimine and diimine oxidation product with max absorbance wavelengths at 350nm and 652nm (Josephy PD et al, 1982). In an acidic environment TMB is oxidized to a yellow diimine with a max absorbance wavelength at 450nm (Josephy PD et al, 1982). The OD at 605nm represents the absorbance of residual color substrate (TMP) not oxidized by HCl (Figure 9).

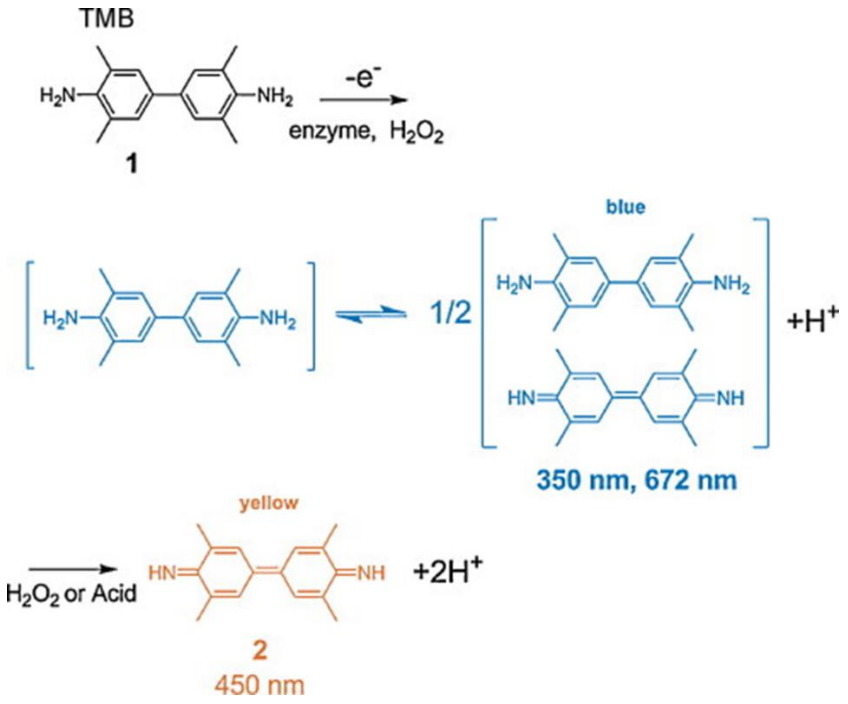

Figure 9. Colorimetric Oxidation of Tetramethylbenzidine TMP used to detect levels of PINP. In a pH neutral environment TMB exists as a pale blue charge-transfer complex of the parent dimine and diimine oxidation product with max absorbance wavelengths at 350nm and 672nm In an acidic environment TMB is oxidized to a yellow diimine with a max absorbance wavelength at 450nm. (Copied from Li B, Du Y, Li T, Dong S, 2009, with permission)

The difference of OD^{605nm} and OD^{450nm} for the calibrators, controls and samples was calculated. A standard curve was created from the OD calibrators as a 4-parameter logistic curve fit by the free online data analysis software: ELSIAanalysis.com. Intact PINP concentration for the samples were calculated based on the regression equation produced from the standard curve. The statistical software *IBM SPSS* was used to perform the Turkey's Least squares significance test and Levene's Test of Equality of Error Variances with help of the RSTATS team at Missouri State University. The concentration of PINP was tested for differences among genotypes using sex as a covariate, differences were considered significant at $p< 0.05$.

Results

The average concentration of PINP for wildtype mice was 13.9 µg/L *(SD=13.4, n=9).* For heterozygous mice, the average concentration was 25.8 µg/L *(SD=30)* (Table 3). No significant difference was observed between the genotypes. Average concentrations were evaluated in male and females to determine if difference exists between the sexs. Average concentration for males were wild-type mice was 11.2 µg/L *(SD=13.2, n=5)* (Table 3). The average concentration for heterozygous mice was 17.6 µg/L *(SD=23.3, n=4).* The PINP concentration for $IDUA^{(-/-)}$ animals was 29.6 µg/L *(28.1, n=6)* (Figure 10). For females the average concentration for wildtype animals was 17.3 µg/L *(SD=14.9, n=4)* and for heterozygous animals was 30.0 µg/L *(SD21.8, n=8).* The average PINP concentration for $IDUA^{(-/-)}$ mice was 3.27 µg/L *(SD=0.77, n=3)* (Table 3, Figure 10). No significance was found between the genotypes using sex as a covariate.

Table 3**.** PINP Statistical Comparison

Sex	Genotype	Average Concentration (ng/L)	Concentration Range	Standard Deviation	Standard Error of Means (SEM)	n
MALE	Wt	11.23	4.01-34.90	13.26	5.93	5
	$HET^{(+/-)}$	17.63	4.66-52.43	23.33	11.67	4
	$IDUA^{(-/-)}$	29.67	3.29-75.85	28.11	11.47	6
FEMALE	WT	17.31	4.39-30.25	14.87	7.43	4
	$HET^{(+/-)}$	29.95	2.87-81.67	21.80	7.71	8
	$IDUA^{(-/-)}$	3.27	2.53-3.66	0.77	0.45	3

A high level of variability was found in all genotypes and sexs as evident by the reported standard deviations (Table 4). Levene's Test of Equality of Error Variances indicated wild-type mice had significantly higher variability than heterozygous and IDUA$^{(-/-)}$ animals.

Discussion and Conclusions

Procollagen Type I N-Terminal Propeptide (PINP) is cleaved from type I procollagen before mature type I collagen can be mineralized into bone tissue. The only source of intact PINP in the serum is that which is cleaved from type I procollagen; therefore the concentration of intact PINP is a biomarker to evaluate levels of bone formation. As mentioned previously, mice with MPS1 have been found to have alterations in the skeletal geometry, microarchitecture, biomechanical properties, and physiochemical properties. Geometric skeletal changes include thicker cortical bone width, increased marrow diameter and decreased femur length. The primary objective of this study was to investigate the source of the altered bone geometry and properties by determining if there were altered levels of bone formation or bone resorption in IDUA deficient mice compared to wild-type mice and heterozygous mice.

There were no significant differences found in the level of PINP across genotypes as determined by the EIA (Figure 12). There was a wide range of concentrations seen in data points. A majority of samples fell between 3 and 10 ng/L of PINP but every other category besides female IDUA$^{(-/-)}$ mice included data points over 30 ng/L and even 80 ng/L (Table 3). Low levels of standard deviation, error and variability reported for the sample population of female IDUA$^{(-/-)}$ mice should not be assumed to be accurate for the total population of female IDUA$^{(-/-)}$ mice due to the low sample number, $n=3$. If the

sample number increased it is assumed the variability would also increase following the trend observed in the wildtype mice, heterozygous mice, and male IDUA$^{(-/-)}$ mice.

The source of variability in the levels of PINP is unclear, but has been previously reported to include the pre-analytical variables including circadian rhythms, fasting state, age, recent fracture and mineral levels. If samples were collected at the same age and in the early morning fasting state the preanalytical variables of circadian rhythms, fasting state and age should have nullified (Schlemmer A., Hassager C., 1999). It is unclear when the sample collection time occurred for experimentation on PINP and TRAP5b. Also estrogen levels were controlled for since all blood serum samples were collected at 4 months of age for mice of the same gender to have similar sexually maturity. Estrogen levels could be different between the sexes, which is the basis for using sex as a covariate. Estrogen plays a significant role in bone homeostasis by inhibiting osteoclast activity (Pacifici R 1996) and having antiapoptotic effects on osteoblasts and osteocytes (Kousteni S. et 2002, Kousteni S. et al 1997 & Emerton K. B. et al 2009). Overall estrogen provides an increase in bone formation and a decrease in bone resorption (Khosla S. et al 2012).

Activity Level. Not all variables influencing bone turnover can be limited by uniform serum collection including physical activity level. Male mice with an IDUA deficiency have been observed to be less active than there wild-type and heterozygous littermates. Bone turnover is directly affected by physical activity (load degree) and it is indirectly affected through the activation of several endocrine molecules such as Interleukin-6 and Interluckin-7 (Lombardi G. et al, 2015). Important questions are, whether higher activity levels may be stimulating bone remodeling or could inactivity be

having an effect on the dynamic relationship between osteoblast, osteoclasts and osteocytes. Activities levels were not quantified, in order to validate this observation activity levels would need to be proved to be significantly different between wild-type mice and IDUA$^{(-/-)}$ mice. The observation of male IDUA deficient mice being less active and less aggressive will be negated if proven false. Another weakness to this argument is it probably cannot be applied to female IDUA$^{(-/-)}$ mice as females are assumed to have similar active levels across genotypes.

Recent fracture. Recent fracture has also been shown to increase bone turnover. One possibility is male wild-type mice higher activity levels leads them to be more aggressive which could result in higher fracture rates. Therefore, if IDUA deficiency resulted in an alteration in bone formation the potential higher activity levels seen in wild-type mice could be masking the difference caused by GAG accumulation. This effect of increased aggressiveness would only be observed in male mice, both wild-type and IDUA females do not typically demonstrate aggressive behavior.

Previous Research. Children with MPS I were found to have increased serum osteocalcin levels with trends of increased serum bone alkaline phosphatase (BSAP) levels compared to age-matched unaffected children (Stevenson D.A. et al 2014), oseocalcin and BSAP are specific to osteoblasts and can be used to compare levels of osteoblast number and activity. Oestreich (2015) suggested there was increased bone formation in children with MPS I, however with compromised function.

Porosity was also observed to be 50% higher in IDUA $^{(-/-)}$ compared to wild-type males by quantitative back scattered electron microscopy (Figure 6). The increase of porosity is assumed to be higher levels of lacunae where osteocytes are located.

Osteocytes are derived from osteoblasts that enclosed itself with newly formed bone tissue. Collectively, previous research demonstrates an increased in osteoblast activity. The increase in osteoblast activity supports the question, why was there not a significant increase in the bone formation marker PINP in IDUA $^{(-/-)}$ mice compared to wild-type? One theory could be the accumulation of GAGs does not alter the signal preceding the secretion of PINP from osteoblasts. Rather the accumulation affects the downstream steps of type I collagen into integration into the bone matrix.

EVALUATION OF BONE REMODELING BY QUANTITATION OF mRNA TRANSCRIPTS

Materials and Methods

RNA isolation. Previously harvested snap frozen tibiae were removed from storage at -80°C and placed on liquid nitrogen. The tibiae (*n=36, 12 for each genotype*) were rapidly crushed with a hammer and homogenized in 500 ml of Denaturing solution (4M guanidinium Thiocyante, 25mM sodiumcitrate, pH 7.0, 0.5% (w/v) Sarkosyl and 0.1M 2-mercaptoethanol) with the MultiGen 7xL homogenizer. Phenol-chloroform extraction was then used to isolate the nucleic acids. Sodium Acetate (2M pH 4.0) was added and the solution mixed by inversion. Acid-phenol:Choloform:Isoamyl (24:24:1) was added, the solution was quickly mixed by vortex, allowed to cool on ice and centrifuged at 4°c until separation of the organic phase and aqueous phase was complete. RNA was precipitated with 500µl of Isopropanol and the supernatant was discarded. RNA was further purified using the Qiagen RNA Isolation Spin Column Kit. Concentration of isolated RNA was quantified by reading the 260nm and 280nm absorbance values using the Nanodrop. (Protocol from Chomozynski and Sacchi, 2006 edited by Arin Kettle Oestreich) Samples (*n=30*) were diluted into 10 µl aliquots containing 2 µg of RNA. RNA was transcribed into cDNA by using Reverse-Transcriptase PCR (Life Technology's High Capacity RNA-to-cDNA kit Lot#00282389). Six of the isolated RNA samples had concentrations less than 2ng which is below the optimal concentration to use for RT-PCR.

Comparative qPCR. SYBR™ Primer/Probes sets were purchased from Applied Biosystems. Cycle Threshold (C_t) is the cycle in which amplification reaches above

background noise, with C_t being inversely related to cDNA is present in the sample. The C_t values for the genes of interest were normalized to the housekeeping genes GAPDH (Glyceraldehyde 3-phosphate dehydrogenase) and PGK1 (Phosphoglycerate Kinase 1). Normalizing genes were verified to have consistent expression in wild-type (*n=2*) and $IDUA^{(-/-)}$ mice (*n=2*) (Table A1). The normalized expression values for heterozygous and $IDUA^{(-/-)}$ are relative to the normalized expression value of wild-type. Expression values were found to be significant if $p>0.05$ uses a two-sided student t-test. (CFX Manager Software Version 3.0) Regulation is the measurement of the change of the relative normalized expression compared to the control (Bio-rad CFX Manager Software guide #10021337).

Agarose Gel Electrophoresis. In order to verify amplification of the correct gene sequence the samples were run on a 1.5% agarose gel to verify the length of the amplicon. The gel was run for 20 minutes at 100 V. To stain the DNA 1.5 µl of SYBERsafe (Catalog # S33102) was added to the gel prior to pouring heated agarose into the casting tray. Gels were imaged with the UV Transillumnator and KODAK (Appendix A1 and T1 A1).

Genotyping. To determine the genotype of the sample numbers for all assays in this study, DNA was extracted and isolated (Lot#SLBL553V)). Amplification using REdMix. Products from PCR amplification were ran on a 1.5 agarose gel with 1.5µl of SYBERsafe. Gels were imaged using the UV transillunator with KODAK image software. Example in Figure A2.

Results

Type I Collagen. Type I collagen was a protein of interest for investigating bone remodeling because it is the major organic component of the extracellular matrix within bone. The normalized expression value for the alpha I chain of Type I collagen for wild-type was 78.3 copies. In heterozygous mice 80.55 copies were seen, and in IDUA $^{(-/-)}$ mice 53.90 copies. Heterozygous mice were found to have 1.02 relative normalized expression to wild-type and IDUA $^{(-/-)}$ mice were found to have 0.6883 relative normalized expression to wild-type (Table 4). Normalized expression values for the alpha II chain of Type I collagen for wild-type was 23.05 copies. In heterozygous mice 29.63 copies were seen and in IDUA $^{(-/-)}$ mice 3.59 copies (Table 4). Heterozygous mice were found to have 1.29 relative normalized expression to wild-type and IDUA $^{(-/-)}$ mice were found to have 163 relative normalized expression to wild-type (Table 4). There was no significant difference found between genotypes for alpha I chain or alpha II chain of type I collagen. (Figure 10).

Colony Stimulating Factor I. Normalized expression values for the CSF-1 for wild-type was 0.1039 copies. In heterozygous mice 0.3697 copies were seen and in IDUA $^{(-/-)}$ mice 0.4693 copies (Table 4). Heterozygous mice were found to have -2.705 relative normalized expression to wild-type ($p=0.0942$) and IDUA $^{(-/-)}$ mice were found to have -2.131 relative normalized expression to wild-type ($p=0.00680$) (Table 4). A decrease expression levels was seen for CSF-1 for IDUA$^{(-/-)}$ mice and heterozygous mice compared to wild-type (Figure 11).

RANK. Normalized expression for RANK for Wild-type mice was found to be 0.1831 copies and for heterozygous mice was 0.0493 copies. Animals deficient in

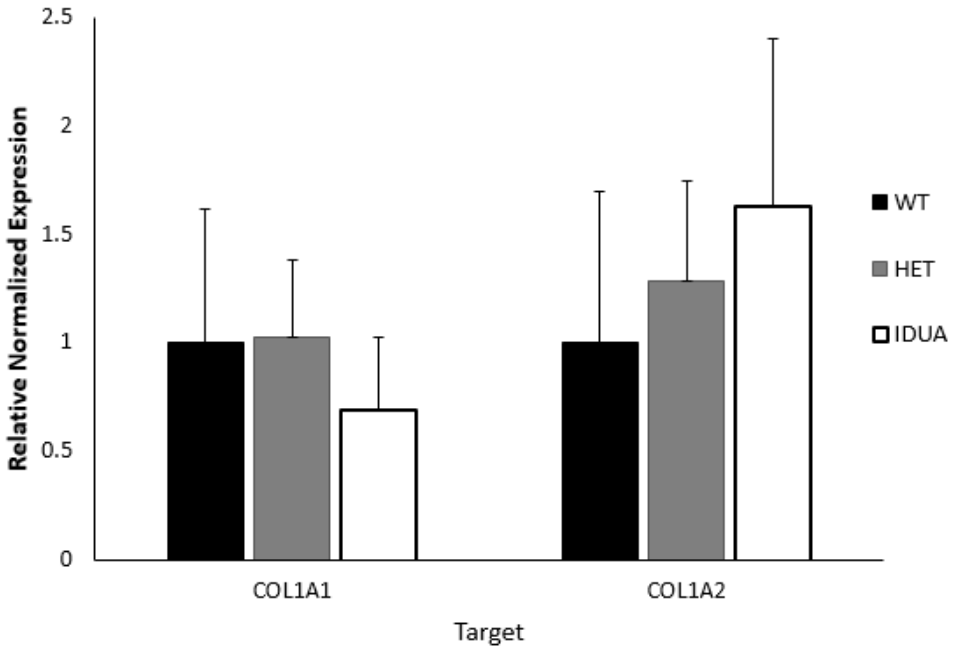

Figure 10. Type I Collagen Expression levels as defined by relative quantification PCR. Total RNA was isolated from tibiae of wild-type (*n=4*), heterozygous (*n=4*), and IDUA$^{(-/-)}$ (*n=4*) mice, transcribed into cDNA and measured for relative expression levels of targets by KAPA PROBE qPCR. Targets included Type I collagen Alpha chain 1 (COlA1) and Type I collagen alpha Chain 2 (COL1A2). Significance was determine if $p < 0.05$ based on one-way student t- test *(CFX Manager Verizon 3.0).*

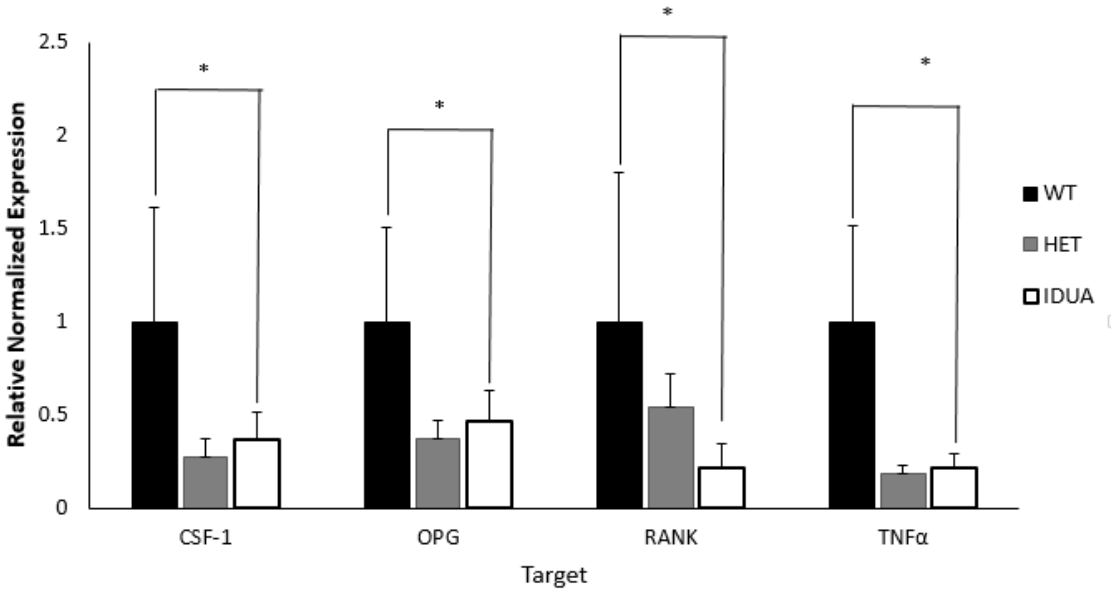

Figure 11. Expression levels for Biomarkers Involved in Osteoclastogenesis as defined by relative quantification PCR. Total RNA was isolated from tibiae of wild-type (*n=4*), heterozygous (*n=4*), and IDUA$^{(-/-)}$ (*n=4*) mice, transcribed into cDNA and measured for relative expression levels of targets by KAPA PROBE qPCR. Targets include, Colony Stimulating Factor-1 (CSF-1), osteoprotegerin (OPG), Receptor Activator of Nuclear Factor κ B (RANK) and Tumor Necrosis Factor α (TNFα). Significance was determine if $p < 0.05$ based on one-way student t- test *(CFX Manager Verizon 3.0).* Asterisks denotes significance difference between heterozygous to wild-type (OPG) or significance difference between heterozygous and IDUA $^{(-/-)}$ as compared to wild-type (CSF-1), (RANK) and (TNFα).

Table 4 Comparison qPCR data. Cycle Threshold values for the genes of interest were normalized to C_t values of the housekeeping genes GAPDH and PGK and made relative to wild-type. A two-way student t-test was used to calculate the significance value. (For $p< 0.05$ to be significant regulation threshold has to be greater than 4 ($R>4$). All testing group ($n=4$).

Target	Genotype	Mean Cq	Normalized Expression	Relative Normalized Expression	Expression SEM	Regulation	P value
COL1A1	Wt	18.14	78.30	1	0.6199	1	1
	HET	15.7	80.55	1.0287	0.3547	1.029	0.00008
	IDUA$^{(-/-)}$	16.7	53.90	0.6883	0.3406	-1.453	0.5237
COL1A2	Wt	19.91	23.05	1	0.6981	1	1
	HET	17.14	29.63	1.2850	0.4613	1.285	0.0050
	IDUA$^{(-/-)}$	17.22	37.59	1.6304	0.7717	1.630	0.8068
RANK	Wt	26.88	0.1831	1	0.6081	1	1
	HET	26.37	0.0493	0.2695	0.1045	-3.711	0.0081
	IDUA$^{(-/-)}$	26.35	0.0668	0.3640	0.1486	-2.740	0.0060
OPG	Wt	29.85	0.0234	1	0.7964	1	1
	HET	28.32	0.0128	0.5443	0.1731	-1.837	0.2486
	IDUA$^{(-/-)}$	30.06	0.0051	0.2181	0.1275	-4.585	0.0574
CSF-1	Wt	27.70	0.1039	1	0.5064	1	1
	HET	26.73	0.0384	0.3697	0.1021	-2.705	0.0942
	IDUA$^{(-/-)}$	26.81	0.0487	0.4693	0.1593	-2.131	0.0068
TNFα	Wt	27.96	0.0869	1	0.5122	1	1
	HET	27.97	0.0163	0.1876	0.0443	-5.332	0.4673
	IDUA$^{(-/-)}$	28.20	0.0186	0.2137	0.0737	-4.679	0.0003

IDUA $^{(-/-)}$ were found to have a normalized expression value of 0.0668 copies. Wildtype expression of RANK was set to 100% of total expression. Expression of heterozygous and IDUA $^{(-/-)}$ were set relative to wildtype expression. Relative normalized expression was found to be 2.705 for heterozygous and 2.131 for IDUA $^{(-/-)}$ (Table 4). A decrease expression levels was seen for RANK for IDUA$^{(-/-)}$ mice and heterozygous mice compared to wild-type (Figure 11).

Osteoprotegerin (OPG). Expression values for OPG were normalized to the housekeeping genes, wild-type mice were found to have 0.0234 copies. Heterozygous mice were found to have 0.0128 copies and IDUA $^{(-/-)}$ mice were found to have 0.0051 copies. Normalized expression values for heterozygous and IDUA $^{(-/-)}$ mice were made relative to wild-type normalized expression values. Heterozygous animals were found to have 0.5443 and IDUA$^{(-/-)}$ animals were found to have 0.2181 relative expression. (Table 4). No change in regulation was seen for heterozygous mice R= -1.837 (*p= 0.2486*) but decrease regulation was observed in IDUA$^{(-/-)}$ mice R= -4.585 (*p= 0.0574*) (Table 4). A decrease expression levels was seen for OPG for IDUA$^{(-/-)}$ mice compared to wild-type (Figure 11).

Tumor Necrosis Factor α (TNFα). Expression values for TNFα were also normalized to the housekeeping genes, wild-type mice were found to have 0.0869 copies. Heterozygous mice were found to have 0.0163 copies and IDUA $^{(-/-)}$ mice were found to have 0.0186 copies. Normalized expression values for heterozygous and IDUA $^{(-/-)}$ mice were made relative to wild-type normalized expression values. Heterozygous animals were found to have 0.1876 expression relative to normalized wild-type expression. Lastly, IDUA$^{(-/-)}$ animals were found to have 0.2181 to normalized. Decreased regulation

was seen in both heterozygous -5.332 (*p= 0.4673*) and IDUA$^{(-/-)}$ -4.679 (*p= 0.0003*) (Table 6). Decrease expression was also seen for TNFα (Figure 11).

Results Summary. No difference was noted between the genotypes for the mRNA levels of COLA1 and COLA2. The mRNA levels for RANK, TNFα, and CSF-1 all showed a decreasing trend for IDUA$^{(-/-)}$ mice and heterozygous mice compared to wild-type, suggesting a decrease in stimulus leading to osteoclastogenesis. Lastly, mRNA levels of OPG were observed to be decreased in IDUA(-/-) deficient mice compared to wild-type mice.

Discussion and Conclusion

Type I Collagen. The main component of the organic matrix of bone is type I collagen, a triple helical protein formed from two α (I) chains and one α (II) chain. Transcript levels of both chains were not observed to be different in heterozygous and IDUA$^{(-/-)}$ mice compared to wild-type as determined by mRNA levels found by qPCR analysis. Various sources have seen an increase in bone mineral density in lysosomal storage disease models compared to nondisease models. As later sources point out the BMD data were not analyzed with body weight as a covariate providing false conclusions about the change in BMD. As mentioned previously, Raman Spectroscopy showed no changes in the Bone Mineral Density Distribution (BMDD) when relating the graylevel (atom number) to calcium content (Figure 5). Calcium is a part of the inorganic material (hydroxyapatite) of bone which attaches at specific areas along Type I collagen. From the collective evidence of Raman Spectroscopy, PINP concentrations determined by ELISA (Table 3) and quantification of Type I collagen mRNA levels (Figure 10) altered

distribution of hydroxyapatite and type I collagen is not a downstream effect of GAG accumulation.

Genes Affecting Osteoclastogenesis (CSF-1, RANK & OPG). Bone remodeling begins with activation of the osteoclasts, including the stimulation of hematopoietic stem cells into osteoclast-precursors and fusion of osteoclast-precursors into multinucleated mature osteoclasts. Survival and proliferation of osteoclast-precursors is dependent on the cytokine CSF-1. This cytokine is also required for the survival of mature osteoclasts and for the cytoskeleton rearrangement needed for polarization of mature osteoclasts. Decreased relative normalized expression was observed to be significant but need not reach above regulated regulation threshold, for both heterozygous (0.3697) and IDUA$^{(-/-)}$ (0.4693) mice compared to wild-type mice (1) (Table 6 and Figure 10). A decrease in CSF-1 would affect the ability of osteoclast-precursors to survive and proliferated into mature osteoclasts, decreasing the tissue's ability to produce actively resorbing osteoclasts.

Osteoblasts and fibroblasts secrete the ligand for RANK (RANKL) into the extracellular matrix where it will bind to RANK located on the surface of osteoclasts. The formation of the RANKL/RANK complex activates a signaling cascade to turn on transcription of genes promoting the fusion of osteoclast-precursors into multinucleated mature osteoclasts. Decreased relative normalized expression was found for both heterozygous (0.2695) and IDUA$^{(-/-)}$ (0.3640) mice compared to wild-type mice (1). A decrease in RANK would affect the ability of osteoclast-precursors to fuse into mature osteoclasts, lowering the number actively resorbing osteoclasts. The lower number of osteoclasts could contribute to the increase in cortical bone width and increased marrow

diameter. Theses changes may contribute to the change in femur geometry suggested compensate for the alterations in the properties of strength.

However, as noted earlier there was not a change in serum levels of TRAP5b between the genotypes indicating no change in the number of osteoclasts. However the use of ELISA to measure TRAP5b may not have the sensitivity required to detect changes between MPS I model and an unaffected model. Which may be accounted for by the observed decrease in relative expression of OPG for IDUA$^{(-/-)}$ (Figure 10), the decoy receptor of RANKL. OPG is used as a control mechanism for stimulation of osteoclastogenesis by blocking the binding of RANKL to RANK. The observed decreased would counteract the decrease seen RANK and possibly CSF-1.

Tumor Necrosis Factor α (TNFα). Finally, mRNA levels of TNFα were seen to be decreased in heterozygous and IDUA$^{(-/-)}$ compared to wild-type. TNFα is believed to reduce bone formation by mature osteoblasts and increase bone resorption by osteoclasts. A decrease in TNFα could suggest increase in bone formation due to inactivation of the bone formation cellular pathways limiting mineralization. Further this could result in a decrease in bone resorption. Notably, the signaling pathways for TNFα are complex and a decrease in mRNA expression could have other effects other than the ones mentioned.

Conclusions and Future Directions

Mucopolysaccharidosis Type I (Hurler Syndrome) devastating lysosomal storage disease resulting in death in early adulthood due to the progressive accumulation of HS and DS. This accumulation is due to a deficiency of producing α-L-iduronidase. Inevitable degeneration of multiple organ systems occurs by mechanisms yet to be fully

understood. Current treatments have been able to decrease the accumulation of GAGs and improve quality of life however progression of dysostosis multiplex continues to worsen. Patients with MPS1 require painful surgery intervention to treat the bone abnormalities despite treatment with enzyme replacement therapy and hematopoietic stem cell transplantation.

The purpose of this study was to investigate bone metabolism between wild-type, heterozygous and $IDUA^{(-/-)}$ mice by analyzing bone remodeling biomarkers. Bone resorption was investigate by analyzing concentrations of PINP and the mRNA concentrations of type I collagen. No significant difference was observed between $IDUA^{(-/-)}$ mice and wildtype for PINP concentrations and mRNA concentrations of alpha I chain and alpha 2 chain of Type I collagen suggesting a deficiency in IDUA does not alter the level of bone formation.

The level of bone resorption was also investigated within this study by analyzing the concentrations of TRAP5b and mRNA concentrations of osteoclastogenesis biomarkers. Those osteoclastogenesis included, Colony Stimulating Factor-1 (CSF-1), osteoprotegerin (OPG), Receptor Activator of Nuclear Factor κ B (RANK) and Tumor Necrosis Factor α (TNFα). No significant difference was found for the concentrations of TRAP5b between the genotypes. However, there was a difference observed between the genotypes for the biomarkers of osteoclastogenesis. The down regulation observed in the mRNA levels in CSF-1, RANK and TNFα indicates decrease osteoclastogenesis since their protein forms stimulate the differentiation of hematopoietic stem cell into osteoclasts. However the down regulation of OPG indicates an increase in osteoclastogenesis since OPG is a decoy receptor for RANK, providing a negative

feedback for osteoclastogenesis. Overall a definitive change in bone resorption due to accumulation of GAG cannot be determined from this study.

To further investigate changes in bone metabolism intracellular signaling pathways should be evaluated. Disruptions in downstream in RANK pathways could be altered by the accumulation of GAG within hematopoietic stem cells and pre-osteoclasts. Secondly, since osteoclasts were seen to have an inability to attach to the bone matrix in a similar lysosomal storage disease (Monroy et al 2002) the molecular interactions involved in the formation the podosomes should be investigated. The binding of β-integrin in osteoclasts to RDG rich proteins located in the bone matrix could be disrupted by the accumulation of GAG. Also the formation of the ruffled border on osteoclasts may be disrupted by the accumulation of GAGs.

REFERENCES

A. Hasilik, E.F. Neufeld, Biosynthesis of lysosomal enzymes in fibroblasts. Phosphorylation of mannose residues. J Biol Chem.255 (1980) 4946–50

A. Schlemmer, C. Hassager, Acute fasting diminishes the circadian rhythm of biochemical markers of bone resorption. Eur J Endocrinol. 140 (1999) 332–337

A. Yoneda, Breast and Ovarian Cancers: A Survey and Possible Roles for the Cell Surface Heparan Sulfate Proteoglycans. Journal of Histochemistry and Cytochemistry 60.1 (2012): 9–21

A.K. Oestreich, M.R. Garcia, X. Yaoc, F.M. Pfeiffer, S. Nobakhti, S. Shefelbine, Y. Wang, A.C. Brodeur, C.L. Phillips, Characterization of the MPS I-H knock-in mouse reveals increased femoral biomechanical integrity with compromised material strength and altered bone geometry Molecular Genetics and Metabolism Reports, 5 (2015) 3–11

B. Clarke, Normal Bone Anatomy and Physiology. Clinical Journal of the American Society of Nephrology : CJASN 3.Suppl 3 (2008): S131–S139

Brandt J., Krogh T.N., Jensen C.H., Frederiksen J.K., Teisner B. "Thermal Instability of the Trimeric Structure of the N-terminal Propeptide of Human Procollagen Type I in Relation to Assay Technology" *Clinical Chemistry* 45.1 (1999) 47-53

C.Y. Li, L.T. Yam, K.W. Lam, Acid phosphatase isoenzyme in human leukocytes in normal and pathologic conditions. J Histochem Cytochem 18 (1970) 473-481

Clarke L.A., Christopher S. Russell Scott Pownall Cara L. Warrington Anita Boro Wski James E. Dimmick Jennifer Toone Frank R. Jirik Murine mucopolysaccharidosis type I: targeted disruption of the murine α-L-iduronidase gene. Human Molecular Genetics 6 (1997)

Coman D.J, Hayes I.M., Collins V, et al. Enzyme replacement therapy for mucopolysaccharidoses: opinions of patients and families. J Pediatr. 152 (2008) 723–7

D. Bauer, J. Krege, N. Lane, E. Leary, C. Libanati, P. Miller, G Myers, S. Silverman, H.W. Vesper, D. Lee, M. Payette, S. Randall National Bone Health Alliance Bone Turnover Marker Project: Current Practices and the Need for US Harmonization, Standardization, and Common Reference Ranges. Osteoporosis International 23.10 (2012) 2425–2433

D. Wang, C. Shukla, X. Liu, T. Schoeb, L.A Clarke, D.M. Bedwell, K.M. Keeling, Characterization of an MPS I-H known-in mouse that carries the nonsense mutation analogous to the Human IDUA-W402X mutation. Molecular Genetics and Metabolism. 99 (2009) 52-71

D.A. Stevenson, K. Rudser, A.Kunin-Batson, E.B. Fung,D.Viskochil, E. Shapiro, Emerton K. B., Hu B., Woo A. A., et al. Osteocyte apoptosis and control of bone resorption following ovariectomy in mice. Bone. 46 (2010) 577–583

E. Kakkis, T. Lester, R. Yang, Successful induction of immune tolerance to enzyme replacement therapy in canine mucopolysaccharidosis I. Proc Natl Acad Sci USA. 101 (2004) 829–34.

Everts V,, Delaissé J.M, Korper W, Jansen DC, Tigchelaar-Gutter W, Saftig P, Beertsen W. "The bone lining cell: its role in cleaning Howship's lacunae and initiating bone formation" Journal of bone Mineral Research 17 (2002) 77-90

F. Boabaid, P. Cerri, E. Katchburian, Apoptotic bone cells may be engulfed by osteoclasts during alveolar bone resorption in young rats. Tissue Cell 33 (2001) 318-25

G. Bach, R. Freidman, B, B. Weissmann, E.F Neufeld, The Defect in the Hurler and Scheie Syndromes: Deficiency of A-L-Iduronidase *Proceedings of the National Academy of Sciences of the United States of America* 69.8 (1972): 2048–2051

G. Lombardi, F. Sanchis-Gomar, S. Perego, V. Sansoni, G. Banfi, Implications of exercise-induced adipo-myokines in bone metabolism. Endocrine NA (2015) 1-22

Genevois K. A., Garin C, Solla F, Guffon N, Kohler R. Surgical management of thoracolumbar kyphosis in mucopolysaccharidosis type 1 in a reference center. *Journal of Inherited Metabolism Disorders*. 37 (2013) 69-78

H. Kaija, S.L. Alatalo, J.M Halleen, Y. Lindqvist, G. Schneider, H.K. Väänänen, P. Vihko, Phosphatase and oxygen radical-generating activities of mammalian purple acid phosphatase are functionally independent. Biochem Biophys Res Commun 292 (2002) 128-132

H.A. Watson, R.J. Holley, K.J. Langford-Smith, F.L. Wilkinson, T.H. van Kuppevelt, R.F. Wynn, B.W. Bigger, Heparan Sulfate Inhibits Hematopoietic Stem and Progenitor Cell Migration and Engraftment in Mucopolysaccharidosis I. The Journal of Biological Chemistry, 289 (2014) 36194–36203

H.C. Anderson, Matrix vesicles and calcification. *Current Rheumatology Reports*. 5 (2003) 222–226

J. E. Wraith, L.A. Clarke, M. Beck, Enzyme replacement therapy for mucopolysaccharidosis I: a randomized, double-blinded, placebo-controlled, multinational study of recombinant human a-L-iduronidase (laronidase). J Pediatr 144 (2004) 581–588

J. Melkko, I. Turid, L. Risteli, J. Pdsteli, B. Smeds, "Clearance of NH2-Terminal Propeptides of Types I and III Procollagen Is a Physiological Function of the Scavenger Receptor in Liver Endothelial Cells." *The Journal of Experimental Medicine* 179.2 (1994): 405–412

J. Tolar, P.J. Orchard. A-L-Iduronidase Therapy for Mucopolysaccharidosis Type I. Biologics : Targets & Therapy 2.4 (2008): 743–751

J. Vääräniemi, J.M. Halleen, K. Kaarlonen, H. Ylipahkala, S.L. Alatalo, G. Andersson, H. Kaija, P. Vihko, H.K. Väänänen, Intracellular machinery for matrix degradation in bone-resorbing osteoclasts. J Bone Miner Res 19 (2004) 1432-1440

J.E. Wraith, Limitations of enzyme replacement therapy: current and future. J. Inherit. Metab. Disorders 29 (2006) 442–447

J.E. Wraith, The first 5 years of clinical experience with laronidase enzyme replacement therapy for mucopolysaccharidosis I. Expert Opin. Pharmacother 6 (2005) 489–506

J.M. Halleen, S.L. Tiitinen, H. Ylipahkala, K.M. Fagerlund, H.K. Väänänen, Tartrate-resistant acid phosphatase 5b (TRACP 5b) as a marker of bone resorption. Clin Lab. 52 (2006) 499-509

J.R. Hobbs, K. Hugh-Jones, A.J. Barrett, Reversal of clinical features of Hurler's disease and biochemical improvement after treatment by bone-marrow transplantation. *Lancet* 2 (1981) 709–712

K. Prydz, Determinants of Glycosaminoglycan (GAG) Structure. Ed. Hans V liegenthart. Biomolecules 5.3 (2015): 2003–2022

K. Shidara , M.Inaba, S. Okuno, S. Yamada, Y. Kumeda, Y.Imanishi, T.Yamakawa, E. Ishimura, Y.Nishizawa, Serum levels of TRAP5b, a new bone resorption marker unaffected by renal dysfunction, as a useful marker of cortical bone loss in hemodialysis patients. Calcif Tissue Int. 82 (2008) 278-87

L. Gilbert, H.E. Xiaofei, P. Farmer, S. Boden, M. Kozlowski, J. Rubin, M.S. Nanes, Inhibition of Osteoblast Differentiation by Tumor Necrosis Factor-α Endroinology 141 (2000) 3956-3963

L. Grigull, K.W. Saykora, A. Tenger, H. Bertram, M. Meyer-Marcotty, H. Hartmann, E. Bultmann, A. Beilken, M. Zivicnjak, M. Mynarek, A.W. Osthaus, R. Schilke, K. Kollewe, T. Lucke, Variable disease progression after successful stem cell transplantation: Prospective follow-up study investigation in eight patients with Hurlers Syndrome *Pediat Transplantation* 2011 (15) 861-869.

L.E, Polgreen, M. Plog, J.D. Schwender, J. Tolar, W. Thomas, P.J. Orchard, B.S. Miller, A. Petryk, Short-term growth hormone treatment in children with Hurler;s syndrome after hematopoietic cell transplantation. Bone Marrow Transplant 44 (2009) 42-49

L.V. Hale, R.J. Galvin, J. Risteli, Y.L. Ma, A.K. Harvey, X. Yang, R.L. Cain, Q. Zeng, C.A. Frolik, M. Sato, A.L. Schmidt, A.G. Geiser, PINP: a serum biomarker of bone formation in the rat. Bone. 40 (2007) 1103-9

M. Koivula, L. Risteli, J. Risteli, Measurment of aminoterminal propeptides of type I collagen (PINP) in serum *Clinical Biochemistry* 45 (2012) 390-927

M. Koivula, V. Ruotsalainen, M. Björkman, S. Nurmenniemi, R. Ikäheimo, K. Savolainen, A. Sorva, J. Risteli, Difference between Total and Intact PINP Annal Clinical Biochemistry 47 (2010) 67-71

M. Mulari, J. Vääräniemi J, H.K.Väänänen, Intracellular membrane trafficking in bone resorbing osteoclasts. Microsc Res Tech. 15 (2003) 496-503

M.A. Monroy, F.P. Ross, S.L. Teitelbaum, M.S. Sands Abnormal osteoclast morphology and bone remodeling in a murine model of a lysosomal storage disease. Bone 30 (2002 352-9

Mizumoto, Shuji, S. Yamada, K. Sugahara. "Mutations in Biosynthetic Enzymes for the Protein Linker Region of Chondroitin/Dermatan/Heparan Sulfate Cause Skeletal and Skin Dysplasias." *BioMed Research International* 2015 (2015): 861752

N.T. Hertel, O. Eklöf, S. Ivarsson, S. Aronson, O. Westphal, I. Sipilä, Growth hormone treatment in 35 prepubertal children with achondroplasia: a five-year dose-response trial. Acta Paediatr. 94 (2005) 1402–1410

P.D. Josephy, T. Eling, R.P. Mason, The Horseradish Peroxidase-catalyzed Oxidationof 3,5,3',5' Tetramethylbenzidine. *J. OF Biological Mistry* April 7 (1982) 3669-4675

R. Florencio-Silva, G Rodrigues da Silva Sasso, E. Sasso-Cerri, M.J. Simões, P. Cerri, Biology of Bone Tissue: Structure, Function, and Factors That Influence Bone Cells. BioMed Research International 2015 (2015) 421746

R. Pacifici, Estrogen, cytokines, and pathogenesis of postmenopausal osteoporosis. Journal of Bone and Mineral Research. 8 (1996) 1043–1051

S. García-López, R.Villanueva, M.C. Meikle. Alterations in the Synthesis of IL-1β, TNF-A, IL-6, and Their Downstream Targets RANKL and OPG by Mouse Calvarial Osteoblasts *In Vitro*: Inhibition of Bone Resorption by Cyclic Mechanical Strain. Frontiers in Endocrinology 4 (2013) 160-168

S. Khosla, M.J. Oursler, D.G. Monroe, Trends Endocrinol Metab. 23 (2012) 576-81

S. Kousteni, J. Reeve, R.W. Shaw, B.S. Noble The death of osteocytes via apoptosis accompanies estrogen withdrawal in human bone. *Endocrine Society Journals and Publications*. 82 (1997) 3128–3135

S. Kousteni, J.R. Chen, T. Bellido, Reversal of bone loss in mice by nongenotropic signaling of sex steroids. *Science*. 298 (2002) 843–846

S. Wilson, S. Saadat Hashamiyan, L. Clarke, P. Saftig, J. Mort, V.M. Dejica, D. Brömme, Glycosaminoglycan-Mediated Loss of Cathepsin K Collagenolytic Activity in MPS I Contributes to Osteoclast and Growth Plate Abnormalities. The American Journal of Pathology 175.5 (2009): 2053–2062

Y. Yoshiko, G.A. Candeliere, N. Maeda, J.E. Aubin, Osteoblast Autonomous P_i Regulation via Pit1 Plays a Role in Bone Mineralization Molecular and Cellular Biology 27.12 (2007) 4465–4474

Yorgan, A. Timur A, T. Schinke, Relevance of Wnt Signaling for Osteoanabolic Therapy. Molecular and cellular therapies 2 (2014) 22-24

APPENDICES

Appendix A.
Length of amplicon in base pairs (Applied Biosystems) Targets included Type I collagen Alpha chain 1 (COlA1), Type I collagen alpha Chain 2 (COL1A2), Colony Stimulating Factor-1 (CSF-1), osteoprotegerin (OPG), Receptor Activator of Nuclear Factor κ B (RANK) and Tumor Necrosis Factor α (TNFα)

GENE	Amplicon Length (bp)
COLA1	89
COLA2	77
CSF-1	70
RANK	65
OPG	75
TNFα	81

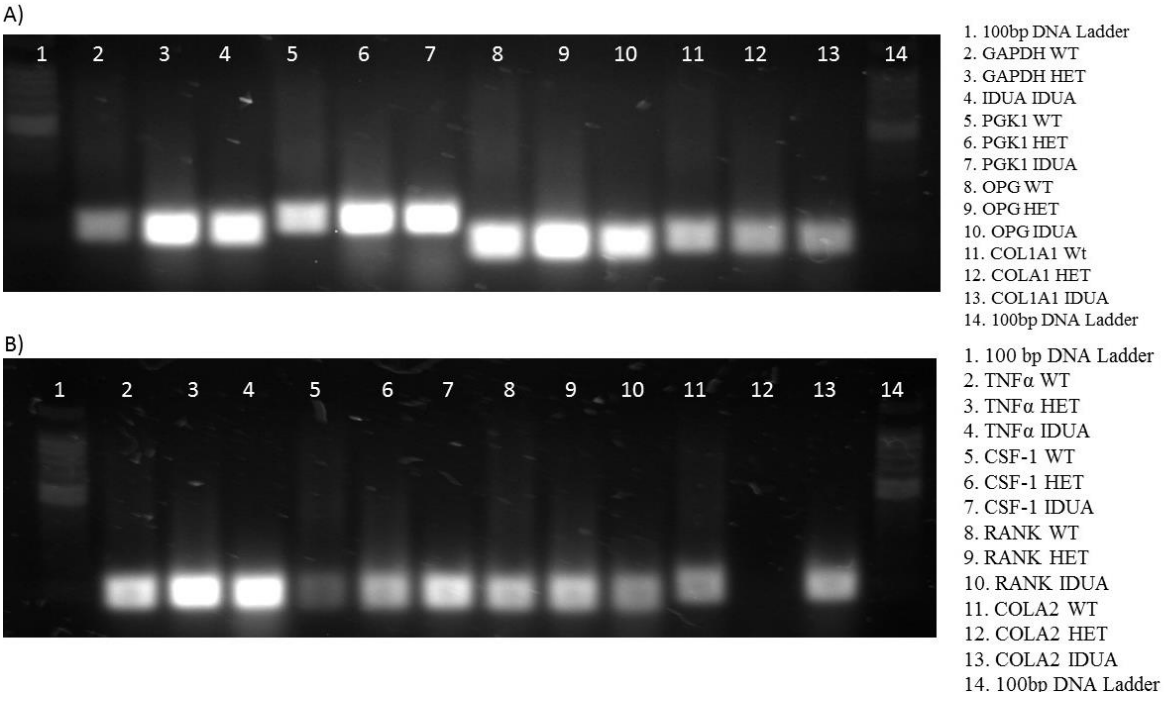

Appendix B Amplicon Length Verification
Products from qPCR were ran on a 1.5% gel with 1.5 µl of Sybersafe to ensure amplification of the correct target A) Targets *GAPDH*, *PGK1, OPG, COLA1, B) TNFα, CSF-1*, *RANK*, and *COLA2*.

Appendix C. Verification of GAPDH and PGK1 as Normalizing Genes for qPCR

Gene	GAPDH	PGK1
Average Ct in Wt	19.33	21.67
Average Ct in IDUA$^{(-/-)}$	18.64	22.3
N	2	2

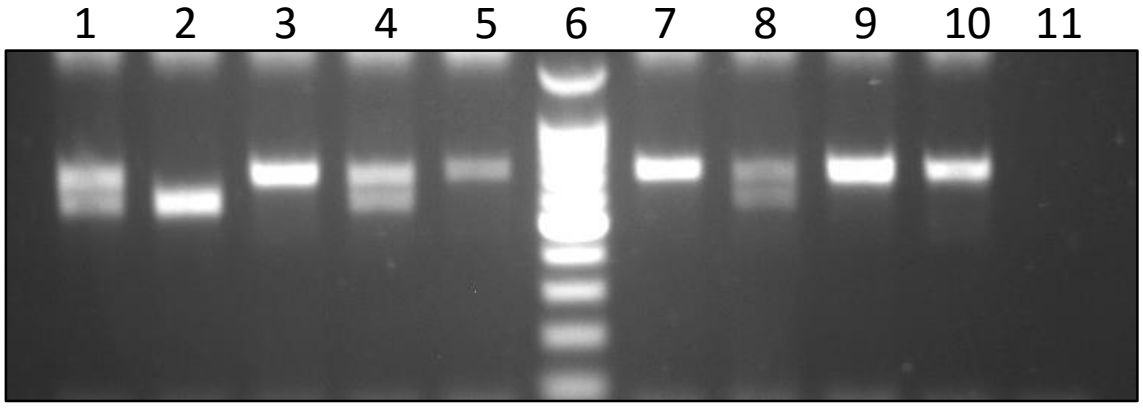

Appendix D.
Genotyping gel Example Samples in order: 405-409, 413-415. Sample 409 was loaded into lanes 9 and 10. A nonmutated allele is 613bp and a IDUA^{-}W392X knockout allele is 576bp. Heterozygous animals will have two distinct bands, wild-type animals had one band at 576bp and IDUA$^{(-/-)}$ animals had one band at 613bp. A 100bp DNA ladder (Promega) was loaded into lane 6 and Lane 11 contains the negative control.